

*Department of Construction Sciences*

Solid Mechanics

ISRN LUTFD2/TFHF-07/5126-SE(1-81)

# INJECTION MOULDING SIMULATION

## -A finite element approach to analyse the thermodynamics in an IM tool

Master's Dissertation by

Rikard Johansson

and

Daniel Konijnendijk

Supervisors

Pär Andersson, Tetra Pak Packaging Solutions AB, Sweden  
Eskil Andreasson, Tetra Pak Packaging Solutions AB, Sweden  
Anders Harrysson, Div. of Solid Mechanics, Lund University, Sweden  
Ulf Nyman, Div. of Solid Mechanics, Lund University, Sweden

Copyright © 2007 by Div. of Solid Mechanics,  
Tetra Pak Packaging Solutions AB, Rikard Johansson, Daniel Konijnendijk  
Printed by Media-Tryck, Lund University, Lund, Sweden

For information, adress:

Division of Solid Mechanics, Lund University, Box 118, SE-221 00 Lund, Sweden  
Homepage: <http://www.solid.lth.se>



# Abstract

Injection moulding, IM, is a common manufacturing method and is used to produce a wide range of plastic products. Tetra Pak uses this method to create the top part of some packages. Trying to shorten the research and development stage, Tetra Pak is interested to investigate the possibility to simulate the manufacturing process of the top part in the FEM software ABAQUS. The FEM approach makes it possible to analyse the thermodynamics within the IM tool and studies could therefore be made to build knowledge of the manufacturing process.

Main objective of this thesis is to create a FE model of the IM tool manufacturing a polymer top, i.e. the top part of the package. Simulated results was evaluated against experimental values measured from an existing IM tool, this to give validity to the FE model. Trough this work careful studies have been made on how diverse parameters influence the simulated results giving a thorough understanding and knowledge of the manufacturing process.

Results from this thesis gave accurate results and an understanding for the thermodynamic in the IM tool, indicating the possibility to simulate the IM process using FEM. However a more careful comparison against the existing IM tool is desirable to ensure that the FE model's results have high accuracy. Studies of the simulated results shows that the polymer top can be manufactured within desired cycle time from a thermal perspective. The FE model also defined the critical areas in the tool design and improvement proposals where created and evaluated. Results from the improved design give guidelines for future work on the IM tool.

**Keywords:** Injection Molding, Finite Element Method, Abaqus, Thermal Analysis.



# Acknowledgement

This master's thesis was carried out at Tetra Pak Packaging Solutions AB in Lund in cooperation with the Division of Solid Mechanics at Lund University during October 2006 to March 2007.

The initiator of this project were MSc Pär Andersson, Tetra Pak Packaging Solutions AB, who also worked as supervisor. We would also like to express our deepest gratitude to our supervisor MSc Eskil Andreasson, Tetra Pak Packaging Solutions AB, for his assistance and devotion. As supervisors they have provided valuable information, helpful technical support and important feedback. Without these two persons this thesis would have been difficult to complete.

We would also like to thank our supervisors at the Division of Solid Mechanics, PhD student Anders Harrysson and PhD Ulf Nyman for their help with the theory, guidance and feedback throughout this project.

A great thanks to the Material Analysis Laboratory at Tetra Pak Packaging Solutions AB for their help with the material properties measurements. Finally we would also like to thank the staff at Tetra Pak in Lund for valuable input and help to the project.

Lund, March 2007

Rikard Johansson

Daniel Konijnendijk



# Nomenclature

|           |               |   |
|-----------|---------------|---|
| $A$       | $[m^2]$       | Area  |
| $C_p$     | $[J/kgK]$     | Specific Heat Capacity at Constant Pressure |
| $K$       | $[J]$         | Kinematic energy                            |
| $L$       | $[m]$         | Length                                      |
| $m$       | $[kg]$        | Mass  |
| $Nu$      |               | Nussels number                              |
| $Pr$      |               | Prandtls number                             |
| $Q$       | $[J]$         | Heat input over time                        |
| $q$       | $[W/m^2]$     | Heat Flux                                   |
| $Re$      |               | Reynolds number                             |
| $T$       | $[^{\circ}C]$ | Temperature                                 |
| $t$       | $[s]$         | Time  |
| $U$       | $[J]$         | Internal energy                             |
| $w$       | $[m/s]$       | Flow velocity                               |
| $x, y, z$ | $[m]$         | Cartesian Coordinates                       |

## Greek Letters

|               |              |                           |
|---------------|--------------|---------------------------|
| $\alpha$      | $[W/m^2K]$   | Heat transfer coefficient |
| $\Delta$      |              | Delta                     |
| $\varepsilon$ |              | Emissivity number         |
| $\lambda$     | $[W/mK]$     | Thermal conductivity      |
| $\mu$         | $[kg/ms]$    | Dynamic viscosity         |
| $\Phi$        | $[W/m^2]$    | Emitted heat radiation    |
| $\rho$        | $[kg/m^3]$   | Density                   |
| $\sigma$      | $[W/m^2K^4]$ | Stefan-Boltzmann constant |
| $\nu$         | $[m^2/s]$    | Kinematic viscosity       |





# Contents

|  |            |
|--|------------|
| <b>Abstract</b>  | <b>iii</b> |
| <b>Acknowledgement</b>                                     | <b>v</b>   |
| <b>Nomenclature</b>  | <b>vii</b> |
| <b>1 Introduction</b>                                      | <b>1</b>   |
| 1.1 Problem Formulation . . . . .                          | 2          |
| 1.2 Objectives . . . . .                                   | 2          |
| 1.3 Limitations and Assumptions . . . . .                  | 2          |
| <b>2 Introduction to Injection Moulding</b>                | <b>5</b>   |
| 2.1 General Injection Moulding . . . . .                   | 5          |
| 2.2 Injection Compressing Moulding at Tetra Pak . . . . .  | 7          |
| <b>3 Theory</b>  | <b>9</b>   |
| 3.1 Introduction to Thermodynamics . . . . .               | 9          |
| 3.2 Constitutive Material Laws . . . . .                   | 11         |
| 3.3 Constitutive Heat Transfer Laws . . . . .              | 12         |
| 3.4 Numeric solution strategy . . . . .                    | 15         |
| <b>4 Finite Element Modeling</b>                           | <b>19</b>  |
| 4.1 Geometry . . . . .                                     | 19         |
| 4.2 Thermal Material Properties . . . . .                  | 21         |
| 4.3 Element Mesh . . . . .                                 | 26         |
| 4.4 Simulation Steps . . . . .                             | 30         |
| 4.5 Surface Interaction and Boundary Conditions . . . . .  | 31         |
| 4.6 Analysis . . . . .                                     | 34         |
| <b>5 Sensitivity Analysis and Verification of FE Model</b> | <b>35</b>  |
| 5.1 Design of Experiments Analysis . . . . .               | 35         |
| 5.2 Experimental tests . . . . .                           | 38         |

|          |   |           |
|----------|---|-----------|
| <b>6</b> | <b>Results</b>  | <b>41</b> |
| 6.1      | FE Simulation of the Injection Moulding Process . . . . . | 41        |
| 6.2      | FE Simulation Using Steel as Tool Material . . . . .      | 44        |
| 6.3      | Energy Balance . . . . .                                  | 46        |
| <b>7</b> | <b>Improvement Proposals</b>                              | <b>49</b> |
| 7.1      | Minimization of Heat Input to the Cavity Tool . . . . .   | 49        |
| 7.2      | Coolant Temperature . . . . .                             | 51        |
| <b>8</b> | <b>Discussion</b>   | <b>53</b> |
| 8.1      | Conclusion . . . . .                                      | 54        |
| 8.2      | Further Work . . . . .                                    | 55        |
| <b>A</b> | <b>ABAQUS/Standard Input File</b>                         | <b>59</b> |

# Chapter 1

## Introduction

Tetra Pak and their customers, e.g. dairies, focus on the packaging costs. Tetra Pak supplies material and the dairies produce several billions of packages every year, this means that reducing milliseconds of the cycle time on every package in production will improve Tetra Pak's position on the market and help both themselves and their customers to increase profit. Simultaneous, in a world of competitiveness, new and inventive package design to end consumers is important for all actors on the packaging market. This means that Tetra Pak has to focus on developing attractive packages to a low competitive cost.

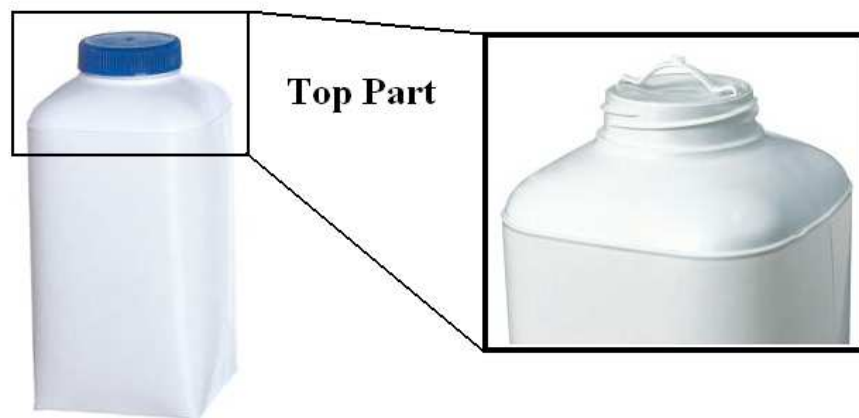


Figure 1.1: 250 ml Tetra Top package with an enlarged top part.

Injection moulding, IM, is a very common manufacturing method and is used to produce a wide range of plastic products [1]. Tetra Pak uses this method to create the top part of some packages, e.g. Tetra Top, cf. Figure 1.1. By combining a paper-based sleeve with a plastic top, highlighted in Figure 1.1, Tetra Pak has a unique and innovative product, perfectly suited for value-added products [2].

## 1.1 Problem Formulation

Injection moulding tools, the mould where the plastic product is produced, is expensive to manufacture, i.e. complex geometry create long machining time at a high cost. Changes in IM tool design and IM tool material is common in the research and development phase and a change means that a new IM tool have to be manufactured, which costs both time and money. Tetra Pak is therefore interested to investigate the possibility to make accurate computer simulations of the plastic top part production process. Changes in IM tool design and IM tool material could then be made before manufacturing the tool and the time to evaluate a new design shortened.

This thesis uses the Finite Element Method, FEM, software ABAQUS v.6.6-1 [3] to simulate the production process of the plastic top. One part of the IM tool, the cavity, is modelled together with the plastic top and other parts considered needed to make accurate simulations. The FEM approach also makes it possible to investigate the thermodynamics within the cavity tool, i.e. the cavity tool is divided into small elements. Studies could therefore be made to find the most critical areas in the cavity tool.

The simulated results in predefined points will be compared with experimental values measured from an existing IM tool. This will give validity to the FEM model and verify the assumptions made and prove the accuracy of the implemented thermal material parameters. When the IM tool is verified and analysed various proposals will be presented to reduce the time needed to produce one polymer top.

## 1.2 Objectives

The purpose of this thesis is to create a FE model and simulate the thermodynamics in the injection moulding process. The thesis will also build knowledge of how a FE model is created and propose various strategies to shorten the cooling time in the injection moulding process technique used at Tetra Pak today.

## 1.3 Limitations and Assumptions

Following limitations and assumptions have been made in this thesis:

- Only one half of the IM tool, the cavity, is modelled.
- No thermal influence on the cavity tool from other parts of the injection moulding pressing unit.
- The core tool and the coolant are assumed to have a defined constant temperature.

- The hot runners are replaced with fixed thermal boundary conditions.
- All heat radiation has been neglected.
- Heat convection from the cavity tool to the surroundings have been neglected.
- No temperature dependent thermal conductivity is used for the plastic top and the cavity tool material.



# Chapter 2

## Introduction to Injection Moulding

Injection moulding, IM, is a common manufacturing technique used for plastic products. The manufacturing technique could be used to produce both small as well as large products in a weight range of 0.000001 kg to 100 kg [1]. The manufacturing process can vary depending on product, this chapter first describes the general IM and then the technique used at Tetra Pak.

### 2.1 General Injection Moulding

An IM machine, also known as press, together with raw plastic material is needed to create a product with the IM technique. The raw material, called resin, is in IM usually shaped as granules. These granules is stored in a feed hopper, a bottom opened bottle which feeds the press with resin, shown in Figure 2.1. The granules need to be molten to enable an injection into the tool cavity chamber, i.e. a cavity that reflects the final shape of the plastic product, the IM machine is therefore equipped with a plasticizing unit in order to melt the resin. Initially in the plasticizing unit a screw, which rotates with help of a motor, melts the granules. Most of the heat is created by friction in the screws rotation but heating bands are often added to supplement the heat generating. When the granules are melted the screw inject the polymer into the cavity chamber with an axial movement.

The tool or mould is the term used to describe the production tooling used to produce a plastic product and consists of at least two parts to permit an extraction of the product. The half in contact with the plasticizing unit is named the cavity and the other half is denoted the core. If the manufactured product have a complex geometry and cannot be formed using only a cavity and a core, moveable sections, named slides, can be used. A clamping force, i.e. a high pressure, is applied to the two halves to eliminate leakage. The applied pressure is generated from a press, usually with a hydraulic or electric driving system. The press can fasten the tool in either a horizontal or vertical orientation.

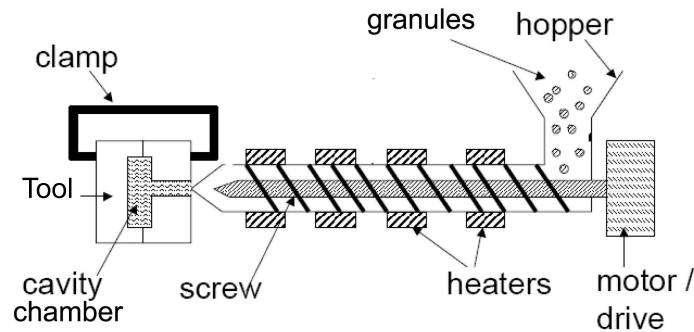


Figure 2.1: General schematic picture of the IM-process [4].

Hardened steel and aluminium is the most common materials used in tools. Hardened steel tools are often more expensive but have a longer lifespan and can therefore produce a higher number of products before the tool is worn. Aluminium is less expensive and has thermal material properties that entail a more efficient cooling but the lifespan is shorter which results in a lower number of products produced compared to steel. The tool will be heated when the molten plastic is injected, to transport the energy from the tool and solidify the plastic the tool usually has drilled cooling channels, often using water as coolant. Improper cooling can result in burnt products or disordered moulding. In recent years research for a more efficient cooling system has resulted in more advanced cooling designs, e.g. milled groove insert [5].

The press, tool, cooling channels, screw, heating bands, feed hopper and resin are all diverse parts of the IM process. The following general steps describe a basic injection cycle:

- The mould is closed shut by a clamping force from the pressing machine.
- A fixed volume of molten plastic is injected, with pressure from the screw, into the mould chamber.
- The cooling channels in the tool cool and solidify the plastic. The solidification starts at the surface of the plastic and when the center is solidified the product is ready to be ejected.
- The mould opens and ejector pins placed within the mould assist in the ejection of the product.



## 2.2 Injection Compressing Moulding at Tetra Pak

At Tetra Pak, a thin walled polymer top made out of High Density PolyEthylene, HDPE, is produced by using injection compressing moulding.

Tetra Pak uses an IM technique where the polymer is heated in the cavity tool with a type of heating band, called hot runner. To eliminate the solidified plastic between the plasticizing unit and the cavity chamber, i.e. a channel through which the plastic flows toward the cavity chamber (the sprue), the hot runner is placed in the cavity tool. In a general IM process this solidified plastic has to be cut or twisted off the manufactured product. By placing the hot runner in the cavity tool, close to the cavity chamber, and regulate the plastic flow with e.g. a gate needle, the plastic between the plasticizing unit and the cavity chamber is eliminated, hence reducing spillage. The warm hot runner placed in the cavity tool with the cold cooling channels creates a conflict between hot and cold. If the cooling channels cool the plastic too efficient in this region the hot runner needs to heat the plastic even more, i.e. more energy is applied to the tool.

Tetra Pak also involves a pressing technique in the IM process. Initially, in the injection part of the cycle the cavity volume is larger than in the cooling part, cf. Figure 2.2. The volume is regulated by the distance between the cavity tool and the core tool. If the distance between these tools decreases the cavity volume will also decrease. One of the advantages of using this pressing method is that there is less distortion in the product when finished.

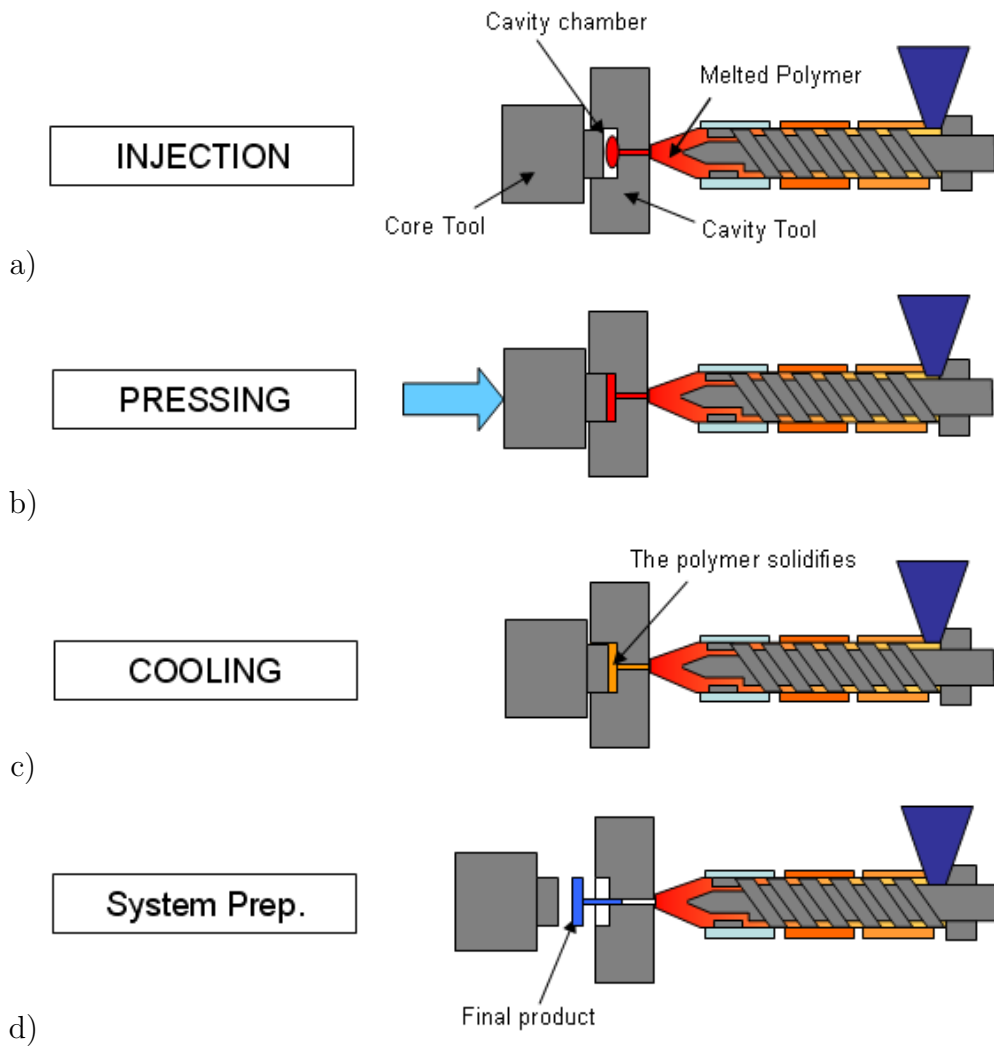


Figure 2.2: The four main events in Injection compression moulding. a) An open cavity in the injection step, b) pressing step, c) cooling step, d) ejection and preparation for a new cycle.

# Chapter 3

## Theory

In this chapter a introduction to thermal theory will be presented. A diverse range of material is used i.e. polymer, aluminium, steel, air and water. Heat flow, both internal and over surface boundaries depends on diverse natural laws. These laws will be translated to numerical solvable equations in the following sections. To be able to make a accurate heat transfer analysis three material properties of good quality is needed, density, specific heat and thermal conductivity.

### 3.1 Introduction to Thermodynamics

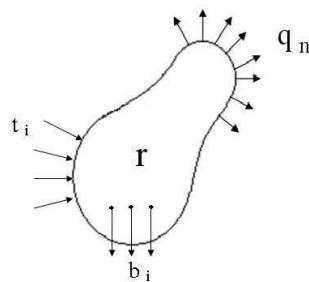


Figure 3.1: Arbitrary body.

Study an arbitrary body, cf. Figure 3.1, which is at rest in a cartesian coordinate system that follows the center of gravity. The mechanical work input  $W$  [ $J$ ] is represented by the traction vector  $t_i$  on the boundary surface respectively the body force per unit volume  $b_i$  acting over the volume on the arbitrary body. The Heat input on the body  $Q$  [ $J$ ] is defined by  $r$  and  $q_n$  which is heat generated within the body, e.g. inductive heating, respectively the heat flow normal to the boundary surface. The arbitrary body can be regarded as a closed system which the first law of thermal dynamics apply to, i.e.

$$\partial K + \partial U = \dot{Q} + \dot{W} \quad (3.1)$$

where  $K$  denote the kinematic energy [ $J$ ] and  $\dot{W}$  is the power input [ $W$ ]. Since the body is at rest and no forces are interacting with the body,  $\partial K = 0$  and  $\dot{W} = 0$ .  $U$  [ $J$ ] which is the internal energy is defined as

$$\partial U = \int \rho u dV \quad (3.2)$$

where  $u$  is the internal energy per unit mass. Furthermore, the rate of heat input is defined as

$$\dot{Q} = \int r dV - \oint q_n dS = \int r dV - \oint q_i n_i dS \quad (3.3)$$

where  $r$  responds to the amount of supplied heat per unit time and volume  $W/m^3$ . The heat flux vector is  $q_i$  [ $W/m^2$ ] and  $n_i$  is the unit vector normal to the boundary. The first law of thermodynamics (3.1) can now be written as

$$\int \rho u dV = \int r dV - \oint q_i n_i dS \quad (3.4)$$

Note that (3.4) is a global equation. To achieve a local form the Gauss divergence theorem [6] can be used.

$$\int \left( \rho \dot{u} - r + \frac{\partial q_i}{\partial x_i} \right) dV = 0 \quad (3.5)$$

Since the volume  $V$  is an arbitrary body, local form of the first law of thermal dynamics is given by

$$\rho \dot{u} = r - \frac{\partial q_i}{\partial x_i} \quad (3.6)$$

and is commonly known as strong form [7]. Weak form can be achieved by multiplying (3.6) with an arbitrary weight function  $w$  and integrate over the body.

$$\int w \rho \dot{u} dV = \int w r dV - \int w \frac{\partial q_i}{\partial x_i} dV \quad (3.7)$$

$$\begin{aligned}\frac{\partial}{\partial x_i}(wq_i) &= q_i \frac{\partial w}{\partial x_i} + w \frac{\partial q_i}{\partial x_i} \Rightarrow \\ \Rightarrow w \frac{\partial q_i}{\partial x_i} &= \frac{\partial}{\partial x_i}(wq_i) - q_i \frac{\partial w}{\partial x_i}\end{aligned}\quad (3.8)$$

Now insert (3.8) into (3.7)

$$\int w \rho \dot{u} dV = \int wr dV - \int \frac{\partial}{\partial x_i}(wq_i) dV + \int \frac{\partial w}{\partial x_i} q_i dV \quad (3.9)$$

By using Gauss divergence theorem on (3.9) it can be transformed into weak form.[6]

$$\int w \rho \dot{u} dV = \int wr dV - \oint w q_i n_i dS + \int \frac{\partial w}{\partial x_i} q_i dV \quad (3.10)$$

It is noted that no assumption of constitutive nature has been made, i.e. (3.10) holds for any choice of constitutive mode.

## 3.2 Constitutive Material Laws

To have any practical use of (3.10) constitutive laws needs to be invoked for  $q_i$ ,  $u$  and  $q_i n_i = q_n$ .  $q_i$  is described with Fouriers law [8]

$$q_i = -K_{ij} \frac{\partial T}{\partial x_j} \quad (3.11)$$

which explain how the heat flow within a body is transported. The assumed constant  $K_{ij}$  is often known as thermal conductivity  $\lambda$  [ $W/mK$ ]. It can be seen through the index of  $K_{ij}$  that the thermal conductivity within a body is not necessarily isotropic. It is assumed that the internal energy only depends on temperature

$$u = u(T) \Rightarrow \dot{u} = \frac{\partial u}{\partial T} \frac{\partial T}{\partial t} \quad (3.12)$$

and describes how much internal energy  $u$  is added due to a change in temperature.  $\partial u / \partial T$  is known as specific heat  $C_P(T)$  [ $J/kgK$ ] for thermal calculations of solid bodies. The index p denotes that constant pressure is assumed [6].

### 3.3 Constitutive Heat Transfer Laws

The constitutive laws for heat transfer through a surface have three different natures [9]:

1. *Conduction*, occurs between solid bodies
2. *Convection*, occurs when fluids or gases are in motion
3. *Radiation*, occurs between two bodies with different temperatures

**Contact conduction** is the ability for two surfaces in contact with each other to transfer heat. To describe the heat flow conditions on the boundaries of the body Newton convection law is used,

$$q_n = \alpha(T - T_\infty) \quad (3.13)$$

The heat flow between two surfaces is described by

$$q_s = \alpha_{conduction}(T_{warm} - T_{cold}) \quad (3.14)$$

where  $\alpha_{conduction}$  [ $W/m^2K$ ] is the surface heat transfer coefficient that depends on physical conditions and material properties for the contact surface, cf. Figure 3.2.

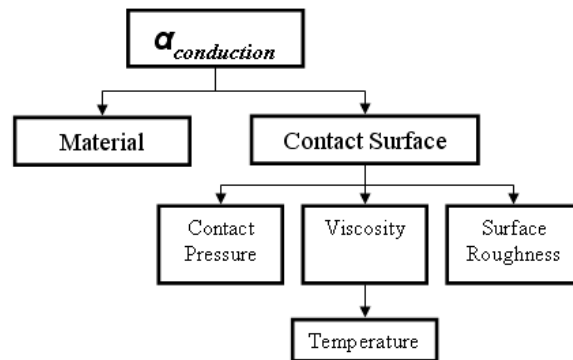


Figure 3.2: Physical condition that effects  $\alpha_{conduction}$ .

There are two types of **convection**, natural and forced. In natural convection the gravity constitute the driving force for the flow and in forced convection the flow is generated by a mechanical force, e.g. a pump. When a fluid is flowing in contact with a surface, e.g. a cooling channel, the surface heat flow depends on the same parameters as contact conduction and is calculated using the same equation as before (3.14). The convection constant  $\alpha_{convection}$  do depend on other physical conditions, cf. Figure 3.3. To determine the convection constant at turbulent pipe flow, both analytical and experimental results are to consider.

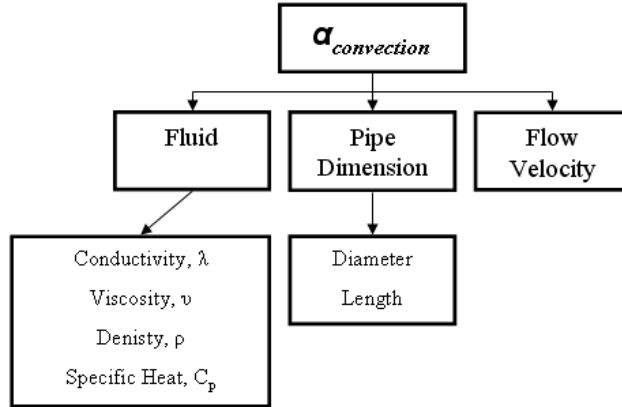


Figure 3.3: Physical condition that effects  $\alpha_{convection}$ .

To determine the  $\alpha_{convection}$  analytically a number of non unit constants has to be defined. When a fluid flows along a surface a boundary layer will be established. In the boundary closest to the wall a laminar layer will exist through which the heat transport will occur by conduction. If the temperature gradient closest to the wall were known the heat transfer could be calculated with fourier's law (3.11). Combined with (3.14) following expression for the heat transfer coefficient,  $\alpha_{convection}$ , is obtained

$$\alpha_{convection} = \lambda \frac{|dT/dx|_{wall}}{\Delta T} \quad (3.15)$$

where

$$\Delta T = T_{warm} - T_{cold} \quad (3.16)$$

Due to the introduction of a absolute temperature gradient in (3.15) no negative number is needed. The temperature gradient is unfortunately often very hard to measure. Experimentally (3.15) is seldom of any use. It is still important for the theoretically understanding of the problem. The temperature gradient along the wall depends on material constants for the fluid and by the surface geometry. This will quickly become a lot of parameters to consider. To simplify this problem a number of non-dimension variables has to be defined. To make (3.15) dimensionless it could be written as

$$\begin{aligned} \alpha_{convection} &= \lambda \frac{|dT/dx|_{wall}}{\Delta T} = \lambda \frac{1}{L} \left| \frac{d(T/\Delta T)}{d(x/L)} \right|_{wall} \Rightarrow \\ &\Rightarrow \frac{\alpha_{convection} L}{\lambda} = \left| \frac{d(T/\Delta T)}{d(x/L)} \right|_{wall} \end{aligned} \quad (3.17)$$

where  $L$  represent the characteristic length [m], e.g. the diameter  $d$  in a pipe. The derivative  $T/\Delta T$  is the temperature variable and  $x/L$  the coordinate variable, both non-dimension. The right side of (3.17) is thus a representation of the temperature derivative at the wall in a non-dimension form. The left side of the equation, i.e.  $\alpha L/\lambda$ , is called the Nussel number

$$Nu = \frac{\alpha_{convection} L}{\lambda} \quad (3.18)$$

Since measuring the temperature derivative at the wall in e.g. a pipe flow is very complicated, the value for  $Nu$  has to be decided in other ways. By using the uniformity laws  $Nu$  can be expressed as a function of different non-dimension units that are easier to calculate. Once (3.18) is defined the heat transfer coefficient  $\alpha_{convection}$  could easily be calculated.

For geometrically uniform systems the basic equation that describes the temperature and velocity fields at forced flow can express the temperature field, in a non-dimension form, as a function of two quantities. Reynolds number

$$Re = \frac{wL}{\nu} \quad (3.19)$$

where  $w$  denotes the flowing velocity [m/s] and  $\nu$  the kinematic viscosity [ $m^2/s$ ]. Prandtl's number

$$Pr = \frac{\mu C_P}{\lambda} \quad (3.20)$$

where  $\mu$  denotes the dynamic viscosity [kg/ms]. The relation between dynamic viscosity and kinematic viscosity is written as  $\nu = \mu/\rho$ . The heat transfer coefficient that is associated with a surface can then be described with (3.18), (3.19) and (3.20) as a function of following type

$$Nu = f(Re, Pr) \quad (3.21)$$

Through work of McAdams among others, the results have been summarized to some simple relations. One, often called the Dittus - Boelters correlation, is

$$Nu = 0.023 Re^{0.8} Pr^{0.4} \quad (3.22)$$

Which is accurate for moderate temperature differences and for flows where  $Re \approx 10\,000 - 120\,000$ , i.e. turbulent flow, and fluids where  $Pr \approx 0.7 - 120$  in channels with the length  $L \geq 60d_i$ , where  $d_i =$  inner diameter. Fluids with moderate viscosity ( $\mu \leq 2\mu_{water}$ ) can usually use equation (3.22) with flows as low as  $Re \geq 3000$ . Material properties is defined



at the fluids average temperature, i.e. the means of the fluid temperatures over a cross-section.

The length of the pipe has an influence on the Nussel number. If the pipe is long the influence is negligible but if it is shorter than  $L \leq 60d_i$  a correction factor should be used.

$$Nu = 0.023Re^{0.8}Pr^{0.4} \underbrace{\left( \frac{1 + (d_i/L)^{0.7}}{1.05} \right)}_{\text{Correction factor}} \quad (3.23)$$

**Heat Radiation** is something all bodies around us emitters and is commonly known as infrared radiation. This radiation is caused by electromagnetic forces generated by the electron in the body.

The heat radiation emitted is strongly dependent on the bodies absolute surface temperature and its characteristics, e.g. colour. A black surface is often considered a perfect radiation surface since it emitters most heat radiation of all surfaces. The emitted heat radiation,  $\Phi_s [W/m^2]$ , from a black surface with the area, A, is according to Stefan-Boltzmann law

$$\Phi_s = \sigma AT^4 \quad (3.24)$$

where T is the surface absolute temperature and  $\sigma$  is Stefan-Boltzmann constant  $[W/m^2K^4]$ .

For regular surfaces the emitted heat radiation is less than for a so called black surface. By using an emissivity number,  $\varepsilon$ , that states the relation between actual emitted radiation from a surface and the radiation from a black surface the heat radiation could be expressed as

$$\Phi_s = \varepsilon\sigma AT^4 \quad (3.25)$$

where  $\varepsilon$  depends on surface material and temperature [10].

## 3.4 Numeric solution strategy

Analytical solutions may exist for simple geometries, this is however often not the case in more complex industrial applications. Therefore, in this section the theories for heat transfer problem will be converted from an analytical to a numerical representation. This due to the complexity of differential equations in most heat transfer problems. The Finite Element Method, FEM, is a common numerical solution model for solving engineering

mechanical problems. Initial the weak form (3.10) has to be transformed into matrix format.

$$\int w \rho i dV = \int w r dV - \oint w q_n dS + \int \nabla(w)^T \mathbf{q} dV \quad (3.26)$$

By assuming a temperature approximation, with help of a shape function  $\mathbf{N}(\mathbf{x})$ , the weak form (3.26) can now be discretized in space. The Galerkin method is used for the selection of weight function.

$$\begin{aligned} \mathbf{T}(\mathbf{x}, t) &= \mathbf{N}(\mathbf{x}) \mathbf{a}(t) \\ \dot{\mathbf{T}}(\mathbf{x}, t) &= \mathbf{N}(\mathbf{x}) \dot{\mathbf{a}}(t) \\ \nabla(\mathbf{T}) &= \mathbf{B}(\mathbf{x}) \mathbf{a}(t) \\ w &= \mathbf{N} \mathbf{c} = \mathbf{c}^T \mathbf{N}^T \\ \nabla(w) &= \mathbf{B} \mathbf{c} \end{aligned}$$

With the above expressions (3.26) can now be written as

$$\mathbf{c}^T \left[ \left( \int \mathbf{N}^T \rho i \right) - \left( - \int \mathbf{N}^T q_n dS + \int \mathbf{N}^T r dV + \int \mathbf{B}^T \mathbf{q} dV \right) \right] \mathbf{c}^T = 0 \quad (3.27)$$

since  $\mathbf{c}$  is arbitrary it follows that

$$\int \mathbf{N}^T \rho i - \int \mathbf{B}^T \mathbf{q} dV = \mathbf{f}_{\text{ext}} \quad (3.28)$$

Since (3.28) is discrete in space but not in time, it is known as the "semi" discrete FE-equation. To make the discretization in time an implicit method is used

$$\dot{u} = \frac{u(T)^{t+\Delta t} - u(t)^t}{\Delta t} \quad (3.29)$$

Inserting (3.29) into (3.28) and using the constitutive law (3.11) for the heat flux  $\mathbf{q}$  results in

$$\begin{aligned} \frac{1}{\Delta t} \int (\mathbf{N}^T \rho u(T)^{t+\Delta t}) dV + \int (\mathbf{B}^T \mathbf{D} \mathbf{B} \mathbf{a}^{t+\Delta t}) dV &= \mathbf{f}_{\text{ext}} + \frac{1}{\Delta t} \int (\mathbf{N}^T \rho u(T)^t) dV \Rightarrow \\ \Rightarrow \frac{1}{\Delta t} \int (\mathbf{N}^T \rho u(T)^{t+\Delta t}) dV + \int (\mathbf{B}^T \mathbf{D} \mathbf{B} \mathbf{a}^{t+\Delta t}) dV &= \mathbf{f}'_{\text{ext}} \end{aligned} \quad (3.30)$$

To solve (3.30) a Newton method is used. For that a residual function needs to be defined.

$$\Psi = \frac{1}{\Delta t} \int (\mathbf{N}^T \rho u(T)^{t+\Delta t}) dV + \int (\mathbf{B}^T \mathbf{D} \mathbf{B} \mathbf{a}^{t+\Delta t}) dV - \mathbf{f}'_{\text{ext}} = 0 \quad (3.31)$$

A standard Newton iteration procedure gives

$$\begin{aligned} \Psi^{i+1} &= \Psi^i + \left( \frac{\partial \Psi}{\partial \mathbf{a}} \right)^i \Delta \mathbf{a} = 0 \\ \Delta \mathbf{a} &= \left( \frac{\partial \Psi^i}{\partial \mathbf{a}^i} \right)^{-1} \Psi^i \\ \mathbf{a}^{i+1} &= \mathbf{a}^i + \Delta \mathbf{a} \end{aligned}$$

where  $i$  indicates the iteration number. For a one-dimensional problem, the essence of the Newton-Raphson strategy is illustrated in Figure 3.4. The problem is to identify the solution to the nonlinear equation  $\Psi(a) = 0$ . A start value  $a^i$  is guessed, at the corresponding point  $\Psi^i$  on the curve  $\Psi(a)$ , the tangent is determined and this tangent is extrapolated to obtain the next estimate  $a^{i+1}$  for the solution. This process is then repeated until the error is within the convergence criteria.

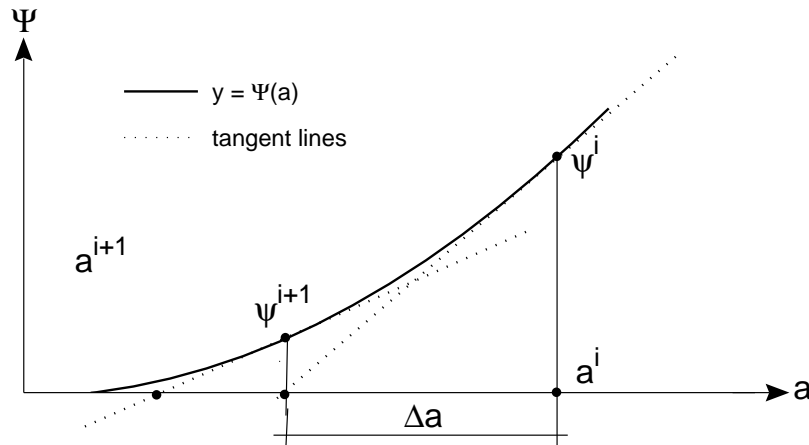


Figure 3.4: Scheme over the Newton raphson method.

The term  $\partial \Psi / \partial \mathbf{a}$  is known as the Jacobi matrix and is in this case given by

$$\frac{1}{\Delta t} \int \mathbf{N}^T \frac{\partial u}{\partial T} \frac{\partial T}{\partial \mathbf{a}} dV + \int \mathbf{B}^T \mathbf{D} \mathbf{B} dV =$$

$$\frac{1}{\Delta t} \int \mathbf{N}^T \frac{\partial u}{\partial T} \mathbf{N} dV + \int \mathbf{B}^T \mathbf{D} \mathbf{B} dV = \frac{\partial \Psi}{\partial \mathbf{a}} \quad (3.32)$$

The heat transfer problem is now converted into a numerical representation [6][7].

# Chapter 4

## Finite Element Modeling

The FE-simulations will be performed in the FE-software ABAQUS 6.6-1 [3]. ABAQUS contains several interacting softwares. A combined pre and post processor consisting of ABAQUS/CAE, short for Complete ABAQUS Environment, which is a graphical environment where models can be created and results viewed. ABAQUS/CAE is divided into ten different modules, e.g. parts, mesh and boundary condition modules, this to facilitate the use of the pre processor. These diverse modules will be explained more in detail further on in this chapter. As an extension to the modelling in order to obtain results a solver has to be used. An implicit solver is most common for uncoupled thermal problems, therefore is the implicit solver ABAQUS/Standard used in the FE simulations.

This chapter describes the modelling procedure for the IM tool. The model consists of seven parts, the core, the cavity, the polymer top and the four polymer volumes between the hot runner and the cavity tool, these parts will be explained thoroughly later on. The cooling channels, placed in the cavity, is not a actual part but needs to be considered in the modelling procedure.

### 4.1 Geometry

The geometry of the polymer top and the cavity tool is imported from the CAD software Pro/ENGINEER as a \*.stp-file in ABAQUS/CAE. Worth mentioning is that a general approach with the SI-units system was used trough the thesis, both in length units and in thermal properties. Simplifications of the geometry were made before the polymer top and the cavity tool was imported. Mainly small details such as holes and round off edges have been eliminated. This was done in order to enable a good mesh quality, minimize the mesh transitions errors and reduce the number of elements.

A boundary condition at the inner surface of the polymer top define the core tool, since the thermal process in the core tool is not included in this assignment. Due to the IM

cycle design contains several core tools, each core tool will have efficient cooling enough to be considered to have a constant temperature.

The four hot runners will not be used in the model. A polymer, HDPE, with variable thickness, interacts between a hot runner and the cavity tool, cf. Figure 4.1. A constant temperature is considered on the surface of the hot runners and therefore could the hot runner be described as a boundary condition on the inner surface of the polymer. Four polymer volumes were designed in Pro/ENGINEER where the inner surface of the polymer reflects the geometry of the hot runner. The polymer volumes will henceforth be named hot runners.

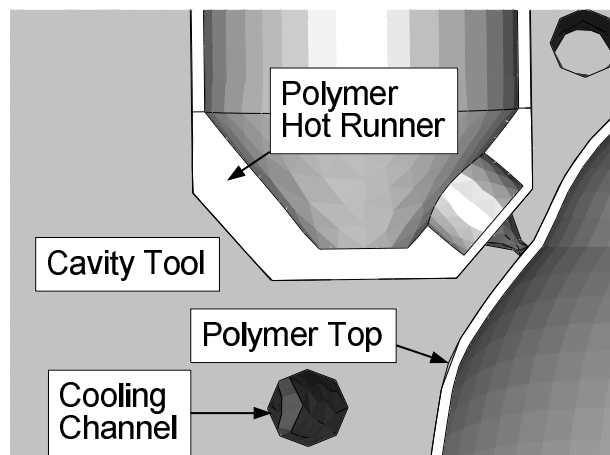


Figure 4.1: A section cut on the FE-modell with all its belonging parts.

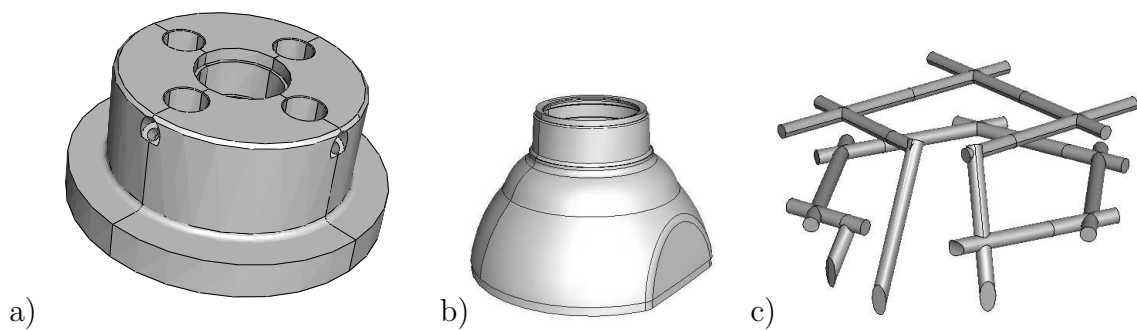


Figure 4.2: Geometry of the parts in the IM system. a) Cavity tool b) Polymer top c) Cooling channels.

The cooling channels have a length of 570 mm and diameter of 5 mm, this will generate a volume of 10 ml. A flow of 7 l/min will give a renewal rate of 0.1 s of the water volume. The weight of the polymer top is small compared to the mass of the cavity tool, shown in Table 4.1.

Table 4.1: Mass and largest diameter of the cavity tool and the polymer top. Volume and largest diameter of the cooling channels

|                  | Cavity tool | Polymer top | Cooling channels           |
|------------------|-------------|-------------|----------------------------|
| Mass / Volume    | ~2.5 kg     | ~10 g       | ~10 ml                     |
| Largest diameter | 170 mm      | ~80 mm      | 5 mm (total length 570 mm) |

## 4.2 Thermal Material Properties

Aluminum is the material used in the IM prototype tool and the polymer top part is made from High Density PolyEthylene, HDPE. Discussions about using steel as tool material have been conducted at Tetra Pak and this section will therefore include steel as an option.

The thermal conductivity,  $\lambda$  [ $J/mK$ ], is the only material property to be considered in a thermal steady state analysis, i.e. when the system have reached equilibrium. Specific heat and density are properties that controls the time needed to reach a steady state level and is used in transient analysis. To illustrate how diverse material properties, e.g. low and high thermal conductivity, affect the thermal behavior an example from the everyday life will be used. Consider a pot on a hot stove, the pot is filled with water, cf. Figure 4.3. For simplicity heat could only move in one dimension and the pot is in perfect contact with the burner, i.e. the temperature at the bottom of the pot is the same as the burner.

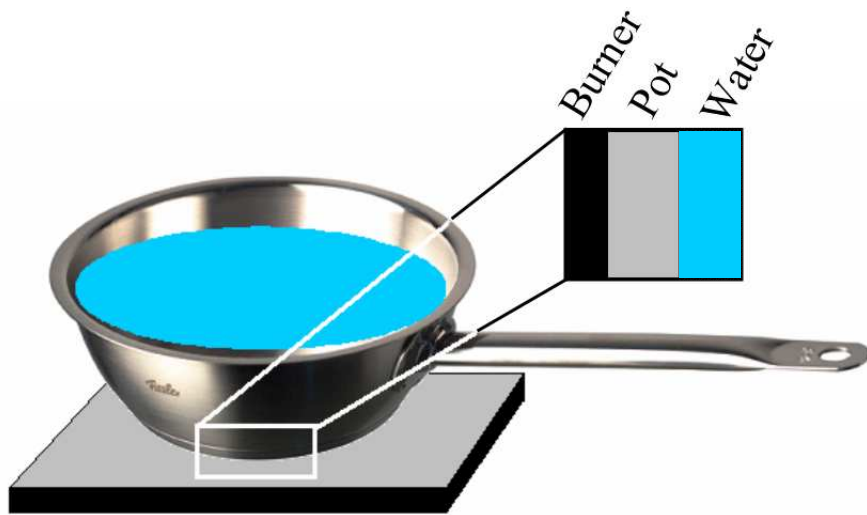


Figure 4.3: Pot on stove, enlarged cut through the pot interacting with burner and water.

In this example the water is continuously replaced in the pot, representing a flow, the temperature of the water is therefore remained constant. The heat flux  $q$  [ $W/m^2$ ], defined in (3.3), is the amount of heat passing through a surface. In steady state analysis  $q_{in}$  equals

$q_{out}$ , cf. Figure 4.4.

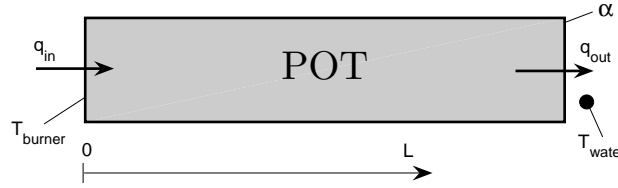


Figure 4.4: Steady state condition where the locations of  $T_{Burner}$ ,  $T_{Pot}$ ,  $T_{Water}$ ,  $\alpha$  and  $L$  is defined.

Using Fouries Law (3.11) and (3.14), the same as for convection, the following expression is obtained

$$q_{in} = \lambda \frac{\Delta T}{L} = \lambda \frac{T_{Burner} - T_{Pot}}{L}, \quad q_{out} = \alpha(T_{Pot} - T_{Water})$$

$$T_{Pot} = \frac{\alpha L T_{Water} + \lambda T_{Burner}}{\alpha L + \lambda} \quad (4.1)$$

By using (4.1) diverse materials temperature gradient could be compared. Figure 4.5 shows three diverse pot materials, aluminium, steel and HDPE. Using HDPE as a pot material may sound strange but remark that this is only an example. The burner heats the outer bottom surface of the pot to 200 °C,  $T_{Burner}$ , and on the inner surface 20 °C water,  $T_{Water}$ , interacts through convection with a heat transfer coefficient,  $\alpha$ , of 5000  $W/m^2K$  on the inner surface of the pot.

The results from Figure 4.5 shows that there is a difference in temperature at  $L=10$  mm between aluminium,  $\lambda = 165 W/mK$  and HDPE,  $\lambda = 0.32 W/mK$ . Which of these three materials is best to use in an IM tool?

The IM tool contains drilled cooling channels. The water in the cooling channels is exposed to heat through convection, same as in the pot. If the temperature gradient between the cooling channels surfaces in the IM tool and the coolant is large, more heat is transferred from the IM tool according to (3.14).

If a point on the IM tool is heated the ideal is that the same amount of heat, i.e. in form of a higher temperature, could be seen at the cooling channels surfaces. If this conclusion is implemented on the results from Figure 4.5 aluminium is most suitable as tool material. This because of the small temperature gradient within the material and thereby generate a large temperature gradient between the cooling channels surfaces in the IM tool and the coolant.

The reader may ask why aluminium has a larger thermal conductivity than HDPE. The thermal conductivity depends on several physical characteristics. Metallic bonds, like in



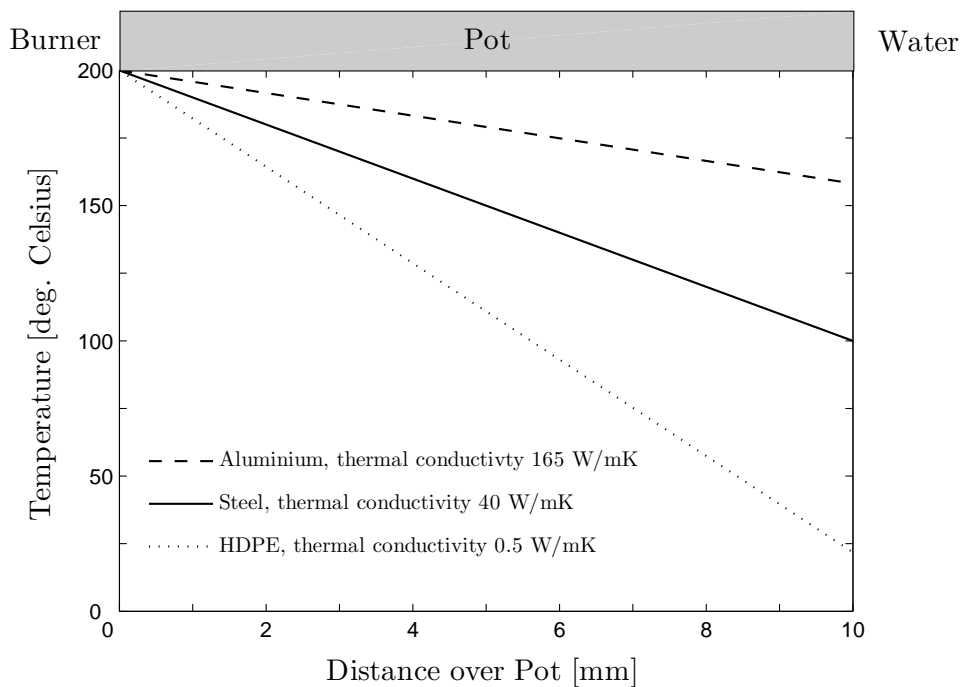
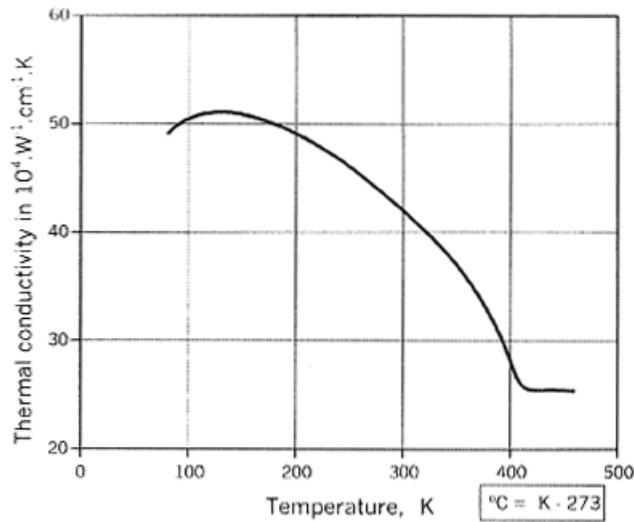


Figure 4.5: Temperature gradient over the pot for three different materials, aluminium, steel and HDPE.

aluminium, enhance the thermal conductivity. A high crystalline atomic structure also increase the thermal conductivity [11]. Aluminium has a crystalline atomic structure, i.e. long-range order of atoms. HDPE is mostly crystalline but the structure also involves an amorphous structure, i.e. no long-range order of atoms, especially at higher temperatures.

The thermal conductivity depends on the temperature and the actual phase, i.e. gas, liquid or solid. A solid phase often implies a higher conductivity than a liquid phase [11]. As a standard in thermal analysis the thermal conductivity are considered as a constant. In Figure 4.6, it is seen that the change in thermal conductivity is relatively small above 400 K, 127 °C. In the analysis the polymer will be cooled down below this temperature but the error using a constant thermal conductivity is considered small. Observe that Figure 4.6 represents a general HDPE. In the analysis the thermal conductivity for HDPE is set to 0.32  $W/mK$  according to measurements at Tetra Pak Packaging Solutions AB laboratory [13]. The temperature level and temperature change in aluminium is considered low compared to the melting point for aluminium hence a constant thermal conductivity is used, i.e. 165  $W/mK$  [14].

The IM process contains changes both in boundary conditions and surface interactions. Therefore is a steady state analysis not possible. In a transient analysis two additional thermal material properties needs to be introduced, density and specific heat.



Conductivity vs temperature of HDPE

Figure 4.6: Thermal conductivity as a function of temperature for a general HDPE [12].

By multiplying the density,  $\rho$ , with the specific heat,  $C_p$ , the amount heat  $Q$  [J] needed to heat one cubic meter one Kelvin is obtained. Table 4.2 shows a comparison between aluminum, steel and HDPE. Steel needs twice as much energy than aluminium to be heated one degree, if the volume is constant.

Table 4.2: Thermal conductivity, density, specific heat and density combined with specific heat for Aluminium, Steel and HDPE in room temperature.

|           | $\lambda$<br>[W/mK] | $\rho$<br>[kg/m <sup>3</sup> ] | $C_p$<br>[J/kgK] | $\rho C_p$<br>[J/m <sup>3</sup> K] |
|-----------|---------------------|--------------------------------|------------------|------------------------------------|
| Aluminium | 165                 | 2830                           | 890*             | $2.5 \cdot 10^6$                   |
| Steel     | 15 – 50             | 7800 – 7900                    | 500 – 630        | $4 – 5 \cdot 10^6$                 |
| HDPE      | 0.32                | 1050                           | 2090*            | $2 \cdot 10^6$                     |

\*temperature dependent data used.

It is complicated to make an analytical calculation of the thermal affect from the density and the specific heat. Using the example with the pot and the FE solver ABAQUS a comparison could be made between aluminium, steel and HDPE. Having a pot with a thickness of 10 mm the temperature of a node, i.e. a point on the pot surface interacting with water, as a function of time, is shown in Figure 4.7. The initial temperature of the pot have been chosen to 50 °C. Starting from  $t = 0$  seconds the pot is in perfect contact with the stoves burner and interacting with water, as earlier.

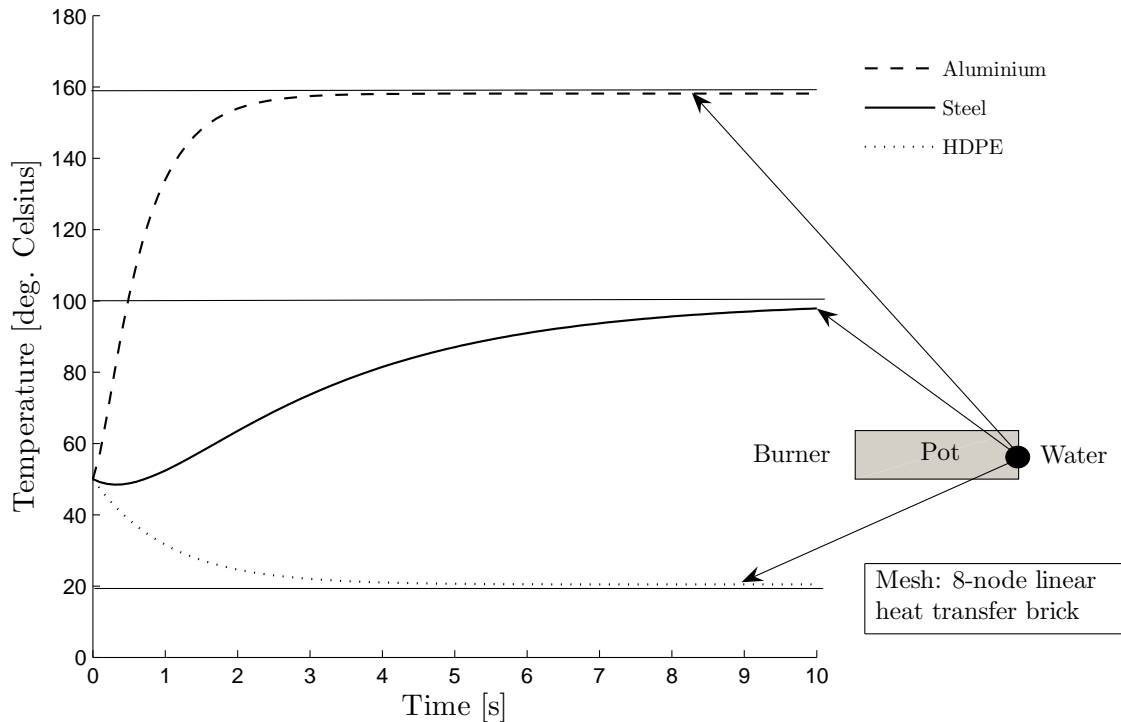


Figure 4.7: FE simulation of a small piece of the pot.

Aluminium and HDPE reaches a steady state level after 3-5 seconds. Steel have however a positive derivative after 10 seconds and therefore not reached a steady state level. A conclusion could therefore be made that a higher specific heat times density increases the time to reach a steady state level. An analogy could be made with a bath sponge placed under a jet of water, with water representing heat. If the bath sponge initially is dry the amount water that flow in to the sponge is not the same as the amount of water leaving the sponge. After some time has passed the water flow into the sponge is the same as the water flow leaving the sponge, i.e. steady state. A high specific heat times density represent a sponge with a large volume and vice versa. A sponge with a large volume needs more time to reach steady state and this is the case for a material with a high density times specific heat.

The thermal conductivity, specific heat and density are all temperature dependent properties. The change in density for the FE simulations temperature interval is considered negligible. Using temperature dependent data of the HDPE density would in this case also result in an error. The geometry used for the HDPE top is calculated for the top's final shape, i.e. at relative low temperature. If a temperature dependent density would have been used with a fixed volume on the polymer top, the mass and therefore also the internal energy, would not be constant during the simulation. Since the density for HDPE increases

with increased temperature the internal energy in the polymer top will be reduced using temperature dependent density.

Specific heat for a material that changes phase, e.g. from liquid to solid phase, is extremely temperature dependent. In the IM process HDPE cools from liquid to solid phase and therefore is temperature dependent data for specific heat of importance. Together with laboratory scientists from Tetra Pak Packaging Solutions AB [13] a temperature dependent specific heat for HDPE was obtained, cf. Figure 4.8.

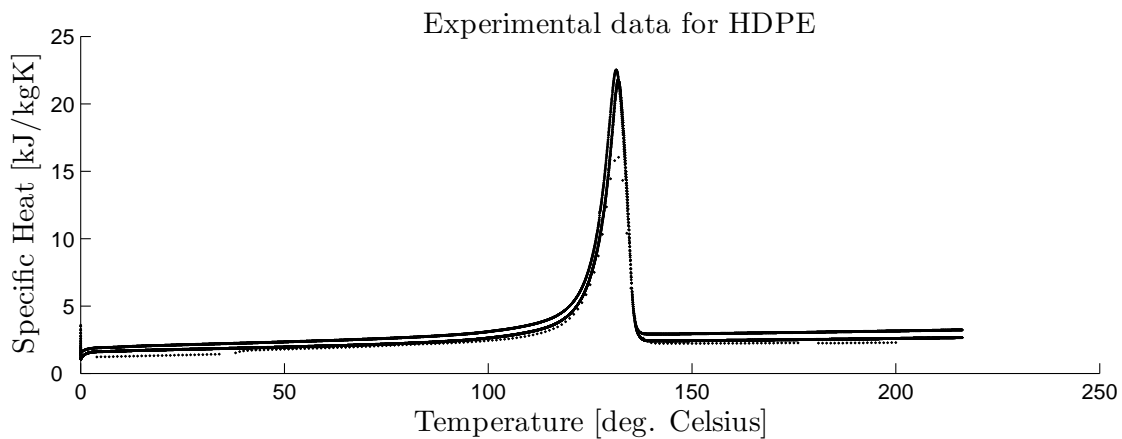


Figure 4.8: Scatter plot of temperature dependent specific heat for HDPE from four samples.

As seen in Figure 4.8, a peak in specific heat occurs at approximately 130 °C. This verifies the importance of using temperature dependent specific heat for HDPE even though the term  $\partial u/\partial T$ , described in (3.12), is included and increases calculation time. 4 samples of HDPE was measured and the difference in internal energy for a fix mass between 80 °C to 200 °C resulted in a 15 % variation between the 4 samples.

### 4.3 Element Mesh

A proper element mesh is very important since the quality of the mesh have a great impact on the accuracy of the results in the analysis. In general an increased number of elements yields a better representation of the geometry and allows for a more enhanced element shape, i.e. no sharp edges etc. A guideline is that more elements improve the accuracy of the results but at the cost of longer calculation time.

The difficulties are to use the most suitable type of elements and finding the point of intersection between an acceptable number of elements and calculation time. In order to be able to design the mesh more effectively some partitions has been made on different

sections of the parts. If a partition of a part is made it will be separated into two cells. Using this, an area of interest are meshed with smaller elements and vice versa and makes the node seeding much more easy on the edges of the various parts and thereby allowing more mesh control. This will also enable results reading at interesting areas of the model.

The element type used to mesh the cavity tool is DC3D8, an 8-node linear heat transfer brick, and DC3D4, a 4-node linear heat transfer tetrahedron [15]. The main problem meshing the cavity tool was to keep the number of elements within an acceptable level. This is due to that the largest part comprises complicated geometry which needs a refined mesh size to be described accurately.

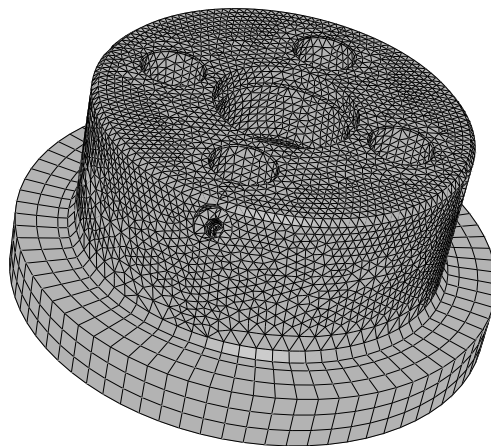


Figure 4.9: Mesh of the cavity tool consisting of 226 771 elements.

Mainly free structured tetrahedron elements in different sizes are used in the complicated areas. On the flange a coarser mesh was used, an assumption was made that this area does not have much influence on the thermodynamics in the IM process. Moreover, since the flange has an uncomplicated geometry, structured brick elements was chosen to save calculation time.

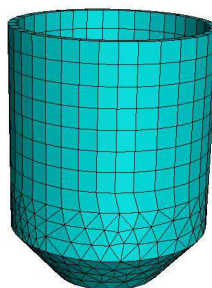


Figure 4.10: Meshed hot runner consisting of 5 210 elements.

The meshing strategy for the hot runners, i.e. the polymer between the actual hot runner and the cavity tool, was equal to the strategy in the cavity tool. The element type used to mesh the hot runners is solid tetrahedron and brick elements. As seen in Figure 4.10 the upper cylindrical part is structurally meshed with brick elements and the lower more complicated geometry freely meshed with tetrahedron elements. Only one element resolution in thickness is necessary since the heat flow of the hot runner flows from the hot inside (high temperature from the hot runner) to the colder cavity tool.

Regarding the top a new mesh strategy had to be formed in order to create a good mesh quality. Three factors have to be considered:

- Cooling from both sides.
- Thin geometry, 0.7 mm.
- Complex geometry.

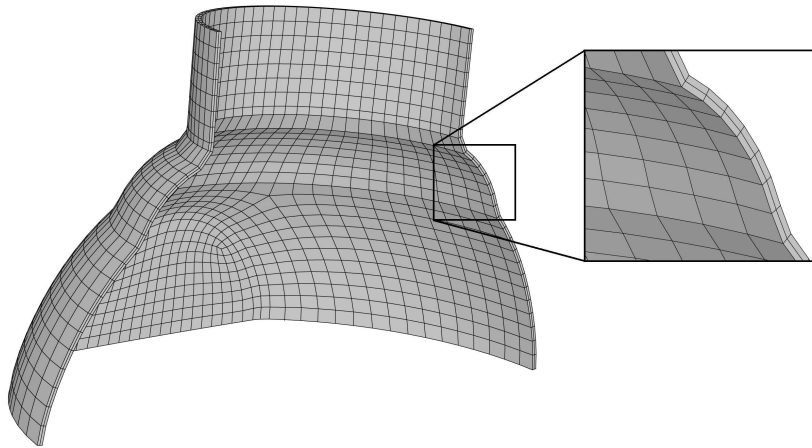


Figure 4.11: Section cut of the meshed polymer top consisting of 4 884 elements. The top have two elements in the thickness direction.

Each of these factors by it self does not cause much problem but in combination they do. Because of a thin and complex geometry the amount of elements needs to be quite high to receive proper quality. The fact that there is cooling from both sides means that the temperature will not be linear within the thickness and a finer resolution in thickness may be needed.

A simple analysis was made to illustrate how the number of elements in thickness direction affects the temperature when cooling from two sides. The heat flow is approximated to be one dimensional due to the fact that the polymer is thin, the thermal conductivity is low and the cooling homogenous. The simple analysis was made by cutting out a small piece, 1x1 mm, of the model in the cavity area and simulate one cycle, cf. Figure 4.12.

Initial, at  $t = 0$  seconds, a 200 °C polymer top is placed between the 50 °C core and cavity

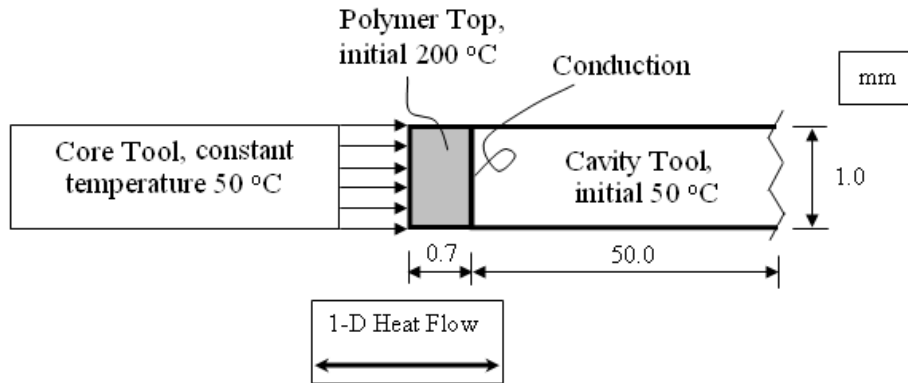


Figure 4.12: Small piece of the polymer top placed between the core and the cavity

tool. During the cycle diverse contact properties is used between the two tools and the polymer. These properties will be explained more in detail further on in this chapter. Simulations with 1, 2 and 15 elements in thickness direction were made. The temperature on the polymer in contact with the core tool for the different simulations is shown in Figure 4.13.

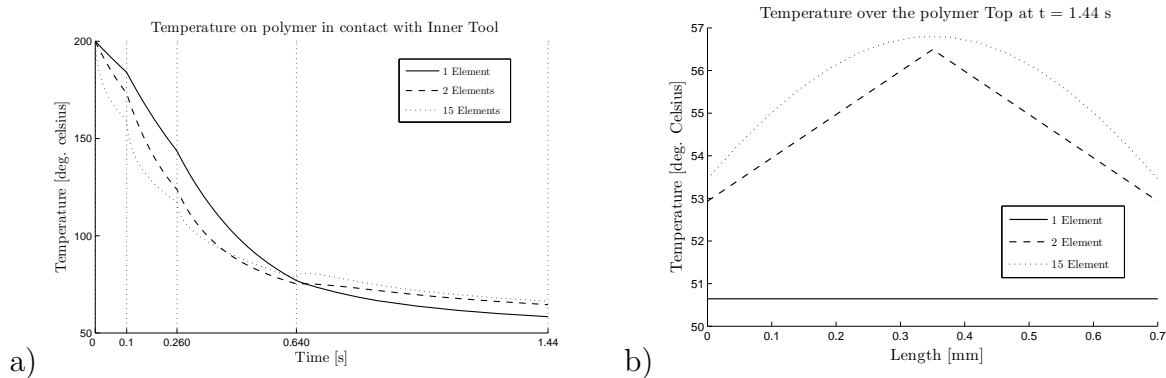


Figure 4.13: Temperature readings a) at contact surface on the polymer. b) through the polymer thickness at  $t = 1.44$  seconds.

The results shows that the difference between having one or two elements have an impact on the final temperature, at  $t = 1.44$  seconds. However, it also shows that the final temperature difference between 2 or 15 elements is small, about 2 %. Initially, the difference between 2 and 15 elements is larger than 2 %, but this error is reduced during the cycle. The resolution over the thickness increases with the increased number of elements. No resolution was obtained using one element but 15 elements resulted in a relative high resolution. Two elements are in this work considered to be accurate enough, this in order to keep the number of elements to a minimum.

A small approximation of the geometry of the polymer top was done. This by creating

a mesh part from the polymer top's outer surface, which resulted in shell elements. By extruding these shell elements, in an inward direction, a solid mesh was obtained with a homogenous thickness of 0.7 mm. The original thickness of the top differs between 0.6 - 0.8 mm. With this method a proper quality mesh of the top, with two elements resolution in thickness, can be created without having to make to big of an approximation.

## 4.4 Simulation Steps

In an IM process a number of different events will occur. As previously explained the polymer is injected into the cavity chamber of the tool, which compress the polymer to its final shape. Then the IM tool cools the polymer to such a temperature level that it has frozen enough to enable a separation from the IM tool. To describe these events in ABAQUS a simulation cycle is divided in steps. In this case the cycle consists of four main steps, cf. Figure 4.14.

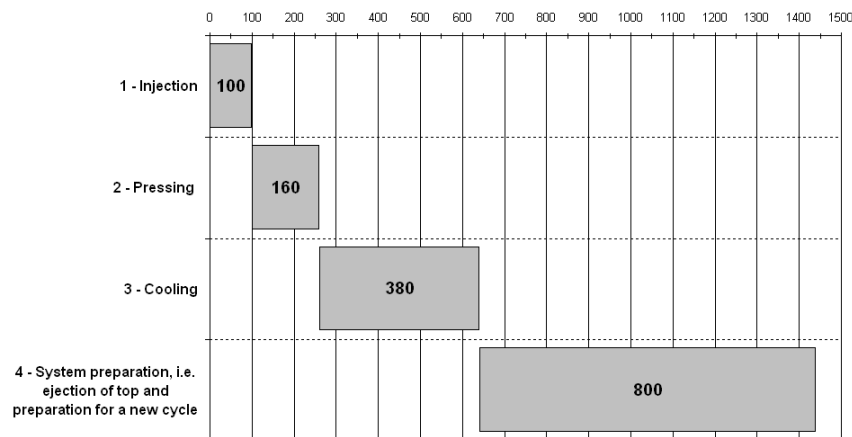


Figure 4.14: Time chart over the steps in a simulation cycle in ABAQUS.

The estimated time period for each step is something that has been decided together with other members of the IM project. Unfortunately boundary conditions and interactions can not be deactivated in one step and then reactivated again in a later step. Due to this fact the defined steps cannot be looped, instead a long string of steps has to be created repeating the same steps over and over to simulate many cycles after each other, cf. Figure 4.15.



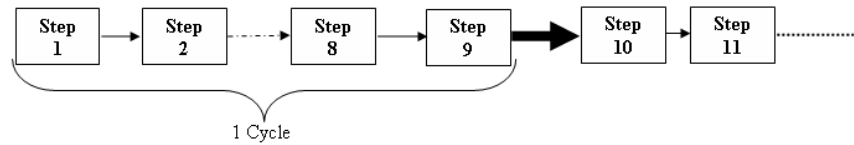


Figure 4.15: Principal scheme on how the steps are run in ABAQUS.

Following steps explains how one cycle is modelled in ABAQUS:

1. *Injection Fix Temp.* A very short step with the only purpose to define a homogenous temperature of 180 °C for the polymer. Duration 0.1 ms.
2. *Injection* represents a real event where the polymer is injected in the moulding cavity for 99 ms.
3. *Substep.* A substep is used when a contact pair is removed. This because ABAQUS/Standard stores the corresponding heat fluxes, for every node on the contact surfaces, and automatically ramps these heat fluxes linearly down to zero during the removal step. This ramping down may have the effect of heating up or cooling down the rest of the body. This problem can be avoided by removing the contact pairs in a very short transient step prior to the rest of the analysis, i.e. a sub step. This step can be done in a single increment [16]. Due to these basic conditions the substeps was set to 0.01 ms.
4. *Pressing* represents the event of the two tools, the core and the cavity, pressing together after the polymer has been injected. This step has a duration of 160 ms.
5. *Substep*, same as item 3.
6. *Cooling*, after the two tool halves are pressed together fully developed cooling exists under a pressure of approximately 600 bar. This step has a duration of 380 ms.
7. *Substep*, same as item 3.
8. *System preparation* represents the cavity tool being removed from the polymer and only cooling from the core tool exist, under less pressure. This step has a duration of 800 ms.
9. *Substep*, same as item 3. This is the last step in the simulation cycle. It will set everything back to zero again, allowing a new cycle to start.

## 4.5 Surface Interaction and Boundary Conditions

To describe what happens between all the diverse surfaces in the model, boundary conditions and interactions has to be defined. In this model there are two different types of

interactions. Contact conductance which is defined with a *gap conductance* and forced convection which is defined with a *film condition* on a surface. These interactions have been defined in section 3.3. The core tool and the cooling water in the cavity tool are represented with a film condition on the polymers inner surface and the surfaces on the cooling channels in the cavity tool. This means that the core tool and the cooling water will be approximated to have a constant temperature, i.e. they can not be heated. This is considered to be a small approximation since the extra time between each cycle the same core tool is used enables an effective cooling. The flow of the cooling water in the cooling channel is of such proportion that the water will not increase much in temperature. If the water flow in the cooling channel is set to 7 l/min it will take 0.1 seconds to replace the volume of water. Convection and heat radiation to the surroundings is in this model not considered. A rough estimate shows that there total effect in heat transfer coefficient is as low as  $20 - 25 \text{ W/m}^2\text{K}$ . Which in contrast to the contact in the cavity and convection in the cooling channel that are in the area of  $2\,400 - 30\,000 \text{ W/m}^2\text{K}$  have a neglectful influence on the results.

Between two surfaces in contact, e.g. the polymer top and the cavity tool, a contact conduction could be specified. The introduced heat transfer coefficient controls the heat flux passing through the two surfaces, described in (3.14). In contrast with a film condition, contact conduction considers the fact that the bodies will be heated or cooled.

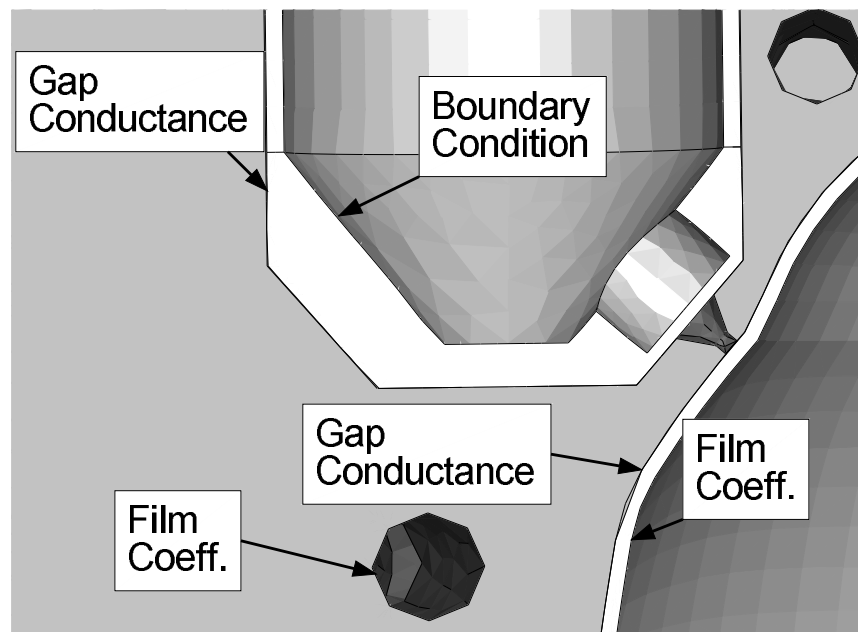


Figure 4.16: Interactions and boundary conditions in FE model.

Initial literature studies and research have set guidelines for the heat transfer coefficients. The ideal would have been to make experiments in a prototype rig to define the values for the heat transfer between the surfaces. But due to the complexity of measuring the

Table 4.3: Heat transfer coefficient  $\alpha_{conductance}$  [ $W/m^2K$ ] at different steps in cavity.

| Step         | Cavity tool<br>Top | Core tool<br>Top |
|--------------|--------------------|------------------|
| Injection    | 800                | 800              |
| Pressing     | 1600               | 1600             |
| Cooling      | 2400               | 2400             |
| System Prep. | 0                  | 1600             |

coefficient, and obtain significant results, a decision was made to use published values. One article, from Kamal M.R. et al [17], uses HDPE as mould material. Another article, from Bendada A. [18], shows that the polymers phase change do not affect the heat transfer coefficient as long as the pressure is high in the cavity. These two articles, together with practical experience at Tetra Pak, work as guidelines for the values of the heat transfer coefficients. During a cycle the conditions will change in the cavity, e.g. pressure and temperature, this will change the heat transfer coefficient as well, cf. Figure 3.2. To solve this problem different values for the coefficients will be set for each step in a cycle. More pressure will induce a higher coefficient and so on.

To decide the heat transfer coefficient for the cooling channels there were more analytical theory to lean on, described in section 3.3. Since the "straight" length of a cooling channel has a great impact on the turbulence, which affects the heat transfer coefficient, it was important to include this in the calculations. Therefore, the cooling channel is divided in sections with different lengths and cross sections, cf. Figure 4.17. For each section of the cooling channel a heat transfer coefficient was calculated, shown in Table 4.4. A decrease in flow velocity generates a heat transfer coefficient decrease.

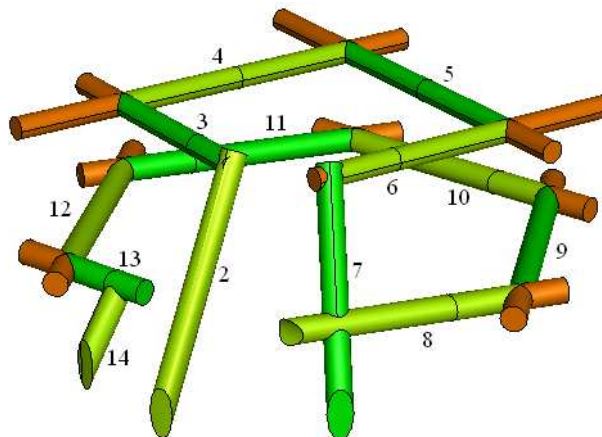


Figure 4.17: Cooling channel divided in sections, orange color represent low flow sections.

Having the cooling channel divided in sections with different lengths the heat transfer

Table 4.4:  $\alpha_{convection}$  [ $kW/m^2K$ ] at different sections in cooling channel.

| Section                            | Low Flow | 2  | 3  | 4  | 5  | 6  | 7  | 8  | 9  | 10 | 11 | 12 | 13 | 14 |
|------------------------------------|----------|----|----|----|----|----|----|----|----|----|----|----|----|----|
| $\alpha_{\dot{V}=5 \text{ l/min}}$ | 5        | 20 | 29 | 28 | 28 | 29 | 22 | 20 | 19 | 19 | 19 | 19 | 23 | 23 |
| $\alpha_{\dot{V}=7 \text{ l/min}}$ | 5        | 26 | 38 | 37 | 37 | 37 | 28 | 26 | 25 | 25 | 25 | 25 | 30 | 30 |

coefficient can be calculated for each section, described in (3.23). The marked ends of each section are here called "low flow" and have an estimated heat transfer coefficient since the flow velocity is unknown.

At the hot runners a boundary condition is set on the inner surface to hold a constant temperature of 200 °C. This condition represents the heat element placed in each hot runner. Due to energy loss from the hot runner to the cavity the temperature has to be set with a margin over the polymers melting point,  $\sim 130$  °C. The polymer top is at the beginning of each cycle given a boundary condition of an initial homogenous temperature, described by item 1 in section "Step". All boundary and interactions are shown in the ABAQUS input file, cf. Appendix A.

## 4.6 Analysis

The average simulation time for one IM-cycle of the complete model consisting of 236 865 elements with 9 steps is three hours. This when using a total of 4 Central Processing Units, CPU, on a Linux-cluster. One cycle represent 1.44 seconds which means that several cycles needs to be simulated until the IM-tool have reached a steady temperature level. To save calculation time a steady state simulation step is initially used. This symbolizes the start up procedure, i.e. when the tool heats up the polymer in the hot-runner and no polymer tops is produced. The steady state step takes less than one hour to simulate.

The use of temperature dependent specific heat increased the simulation time with approximately 200 %. The temperature dependency also made it impossible to use fix time steps, this resulted in non convergence solutions. Fix time increment is a convenient way of controlling the simulations and receive results in high frequency at interesting times. The affect that temperature dependent specific heat have on the result is however larger than not using fix time steps.

# Chapter 5

## Sensitivity Analysis and Verification of FE Model

When results from the simulations was obtained, questions like "how the heat transfer coefficient in the injection step affect the temperature of the polymer top?", "is this temperature plausible?" etc occurred. A Design Of Experiments, DOE, analysis of the cavity and experiments in the prototype rig was therefore performed to evaluate the FE model.

### 5.1 Design of Experiments Analysis

The only heat transfer coefficient value found in published articles was for the polymer HDPE at fully developed cooling. As previously mentioned the FE model is designed with several different simulation steps and diverse magnitudes for the heat transfer coefficient between the cavity tool and the polymer top. Numerical values for these different simulation steps where set together with Pär Andersson, an expert on In-Line Plastic Moulding at Tetra Pak Packaging Solutions AB.

A DOE was made to evaluate how the values for the heat transfer coefficient in the diverse steps affect the temperature inside and on the polymer top's susrface. This was made by using the values from Table 4.3 and set high and low values out of these, shown in Table 5.1.

In the injection step a high value of the heat transfer coefficient represent a fully developed cooling with compensation for that only about half of the cavity chamber is in contact with the polymer (no pressing has occurred). The low value of the heat transfer coefficient in the injection step is then set so the base line value represent the average of high and low. In the pressing step the high value represent the fact that a fully developed cooling could be possible, low is set with the same method as before, i.e. baseline is an average of high and low. The values in the system preparation step are set in the same manner. Observe

Table 5.1: Low, baseline and high values for the heat transfer coefficient in the cavity [ $W/m^2K$ ].

|                    | Low  | Baseline | High |
|--------------------|------|----------|------|
| Injection          | 400  | 800      | 1200 |
| Pressing           | 800  | 1600     | 2400 |
| Cooling            | 1200 | 2400     | 3600 |
| System Preparation | 800  | 1600     | 2400 |

that the cavity tool does not interact with the top in this step and values are therefore only changed for the core tool. Finally, values for high and low is set in the cooling step with the same percentage increase and decrease as previous simulation steps. A 2-level full factorial design is now established for the heat transfer coefficients in the cavity.

16 simulations is needed to make a 2-level full factorial design for four diverse control factors , i.e.  $2^4 = 16$ . The statistical program MINITAB [19] was used to make systemized simulations. MINITAB helps the user with input to each simulation and also evaluates the results in a convenient way. The FE model of the simulations is structured as mentioned in the previous chapter. The temperature of the water in the cooling channels is set to 50 °C and the flow to 7 l/min. Only one cycle was simulated to save simulation time, i.e. total time 1.44 seconds in reality, simulation time is 3 hours. Therefore are the magnitudes of the results not comparable with a continuous IM process, but one cycle is considered enough to make conclusions of how each part of the cycle, i.e. injection, pressing, cooling and system preparation, affect the final temperature.

Three node temperatures in the injection region of the top was selected as response parameters, cf. Figure 5.1. One node at the outer surface, one in the center and one at the inner surface facing the core tool.

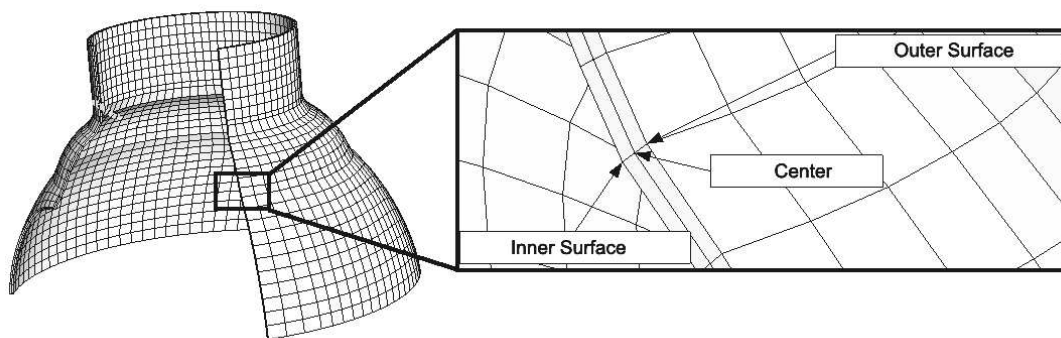


Figure 5.1: Selected result nodes on the polymer top.

These three temperatures is selected after one cycle is completed, i.e. after 1.44 seconds. Figure 5.2 shows a main effect plot of how a change in heat transfer coefficient affect

the final temperature in the diverse nodes. The four different steps is represented with a figure, the temperature for the diverse nodes could be seen on the vertical axis and the heat transfer coefficients from Table 5.1 on the horizontal axis.

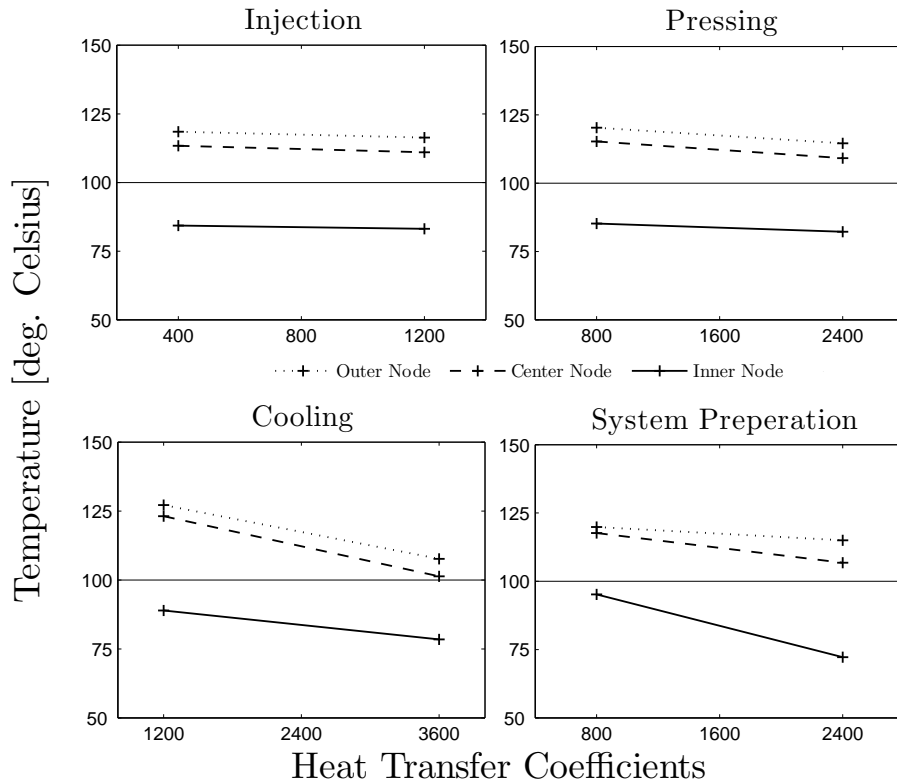


Figure 5.2: Main effect plot on how the heat transfer coefficient in the cavity affect the polymer top temperature.

A small gradient means that the heat transfer coefficient have low influence on the temperature and vice versa. As seen in Figure 5.2, step injection, the temperature for the outer, center and inner node is almost the same for both a heat transfer coefficient of  $400 W/m^2K$  and  $1200 W/m^2K$ . The same tendency could be seen in the pressing step. The injection and the pressing step have therefore a low influence on the final temperature of the top. The heat transfer coefficient for the cooling step affect the final temperature the most, i.e. a large gradient. In the system preparation step the node on the inner surface is to a larger extent affected by a heat transfer coefficient change than a node on the outer surface. This is a distance effect. The heat transfer coefficient on the outer surface in the system preparation part is always zero. Since the polymer top have a low thermal conductivity a change in temperature some distance away, e.g. at the inner surface of the polymer, is of low influence.

Since the values for the heat transfer coefficients in the injection and pressing step have low influence on the final result these steps are of low importance for the FE model. The

certainty of the results also increases due to that the values for the heat transfer coefficient in the injection and pressing step was set with help of experienced persons.

## 5.2 Experimental tests

Experimental tests were made in the prototype rig to verify the simulation results. By measuring temperatures at different locations on the prototype cavity tool these temperatures could be compared to the temperatures at the same location in the simulated IM tool. Due to the complexity of measuring the temperature during a cycle a choice was made to make the measurements when only the hot runners and the cooling channels were running. This choice eliminates the possibility to verify the heat transfer from the polymer top, but the verification of the heat transfer from the polymer top was made in the design of experiment.

A FLUKE 52 thermometer together with a thermocouple type K was used to measure the temperature on the cavity tool, cf. Figure 5.3. The test equipment was calibrated at 60 °C according to EAL publication EA/4-02 [20]. This resulted in an uncertainty of  $\pm 0.6$  °C on the results from the test equipment.

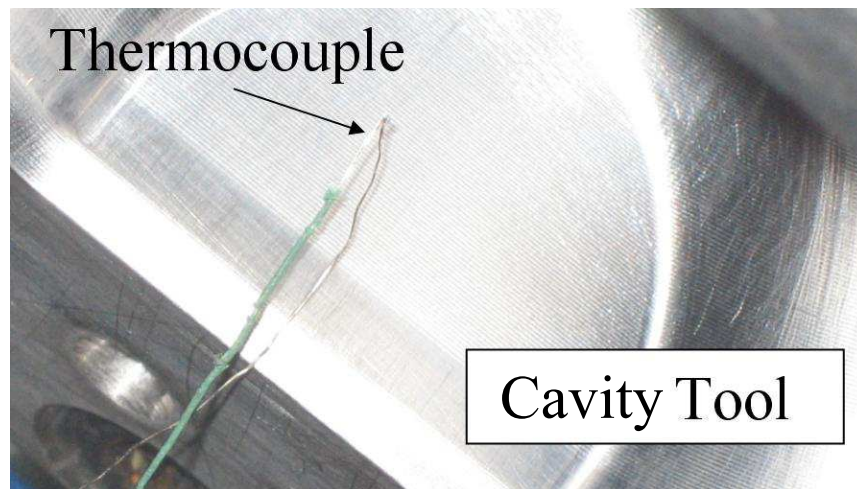


Figure 5.3: The thermocouple placed in the cavity.

Temperatures from five different locations on the cavity tool was measured, at one injection hole, between two injection holes, on the flat lower side of the cavity, on the flange at the cooling inlet and on a the flange at the opposite side of the tool, cf. Figure 5.4.

The current settings from the rig, i.e. hot runner temperature (300 °C), cooling flow (5 l/min) and cooling temperature (50 °C), was then implemented in the FE model. By changing the heat transfer coefficients, between the hot runners/cavity tool and the cooling channels, with  $\pm 20$  % a temperature interval was created.



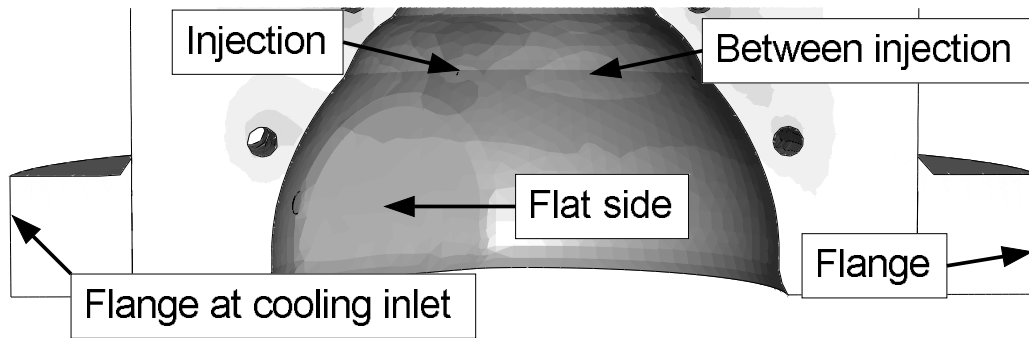


Figure 5.4: Schematic picture of the five locations where the temperature was measured.

A 20 % increase of the heat transfer coefficient for the hot runners and a 20 % decrease of the heat transfer coefficient for the cooling channels enables a higher energy transportation to the cavity tool and less energy transportation from the cavity tool resulting in a higher temperature. Vice versa, a 20 % decrease of the heat transfer coefficient in the hot runners and a 20 % increase of the heat transfer coefficient in the cooling channels enables a higher energy transportation from the cavity tool and less to the cavity tool. These two scenarios are considered a worst/best case. Figure 5.5 shows a scatter plot of the experimental measured locations and the same five locations from the simulated best and worst cases.

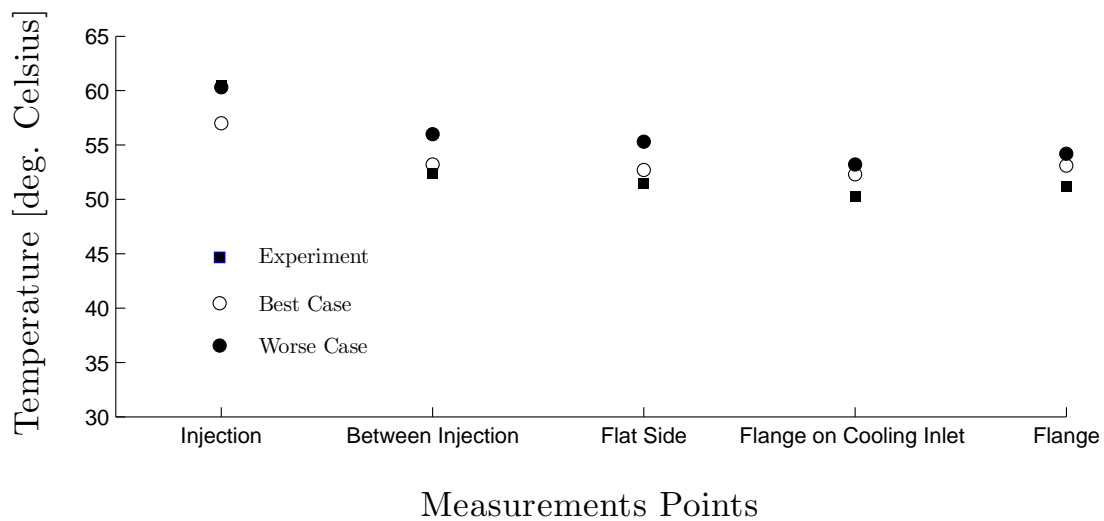


Figure 5.5: Scatter plot of the experimental and simulated results from the five different locations.

The temperatures from the worst case are higher than the best case in all five locations. The difference between worst and best is lower at the flange. This is because of the distance between the hot runner region, where the increase and decrease of the heat transfer coefficients is made, and the flange. The measured temperatures from the rig are lower than

the best case in all measured locations except at the injection location. It is complicated to measure an accurate temperature and even though a calibrated equipment was used a lot of other reasons could result in measurement errors. This experiment has given a guideline that the results from the simulation are in same level as the prototype rig, although not 100 % correct.

# Chapter 6

## Results

Ten injection moulding cycles are simulated to evaluate when the cavity tool and the injection moulding process reaches a steady temperature level. Steady temperature level is in this chapter defined by the final temperature after each cycle. The results are then explained to give an understanding of the thermodynamics in the IM process. A change in cavity tool material, from aluminium to steel, is made and comparisons of results are demonstrated. An energy balance is made to analyse how much energy that is applied and removed from the cavity tool.

### 6.1 FE Simulation of the Injection Moulding Process

This simulation consist of 10 IM cycles, i.e. the production of 10 polymer tops. The total simulation time for 10 cycles was 30 hours. The coolant temperature is set to 25 °C, compared to the 50 °C used in the experiment, cf. section 5.2. The coolant flow is increased to 7 l/min, compared to 5 l/min used in the experiment. These settings are more likely to be used in a continuous IM process. Coolant temperatures under 25 °C may cause condensation in the IM process area which is not preferable from an aseptic point of view.

A survey over the temperatures in the system is important for the understanding of the thermodynamics in the IM process. Figure 6.1 shows a section cut of the cavity tool immediately at the end of the 10th cycle. The highest temperatures in the cavity tool could be seen around the injection hole, this area is hence the most critical in the cavity tool. During a cycle the temperature for this area can increase to  $\sim 40$  °C. As seen in Figure 6.1 the temperature varies from 34 °C to 26 °C, i.e. 1 °C to 9 °C over the coolant temperature. These results could be compared to the experimental measurements, seen in Figure 5.5, with coolant temperature of 50 °C, lower coolant flow (5 l/min instead of 7 l/min) and a higher hot runner temperature (300 °C instead of 200 °C). The experimental measurement shows an increased temperature of 11 °C to 1 °C over the coolant temperature. The

temperature on the opposite side of the two cooling channels is low and is therefore of small interest.

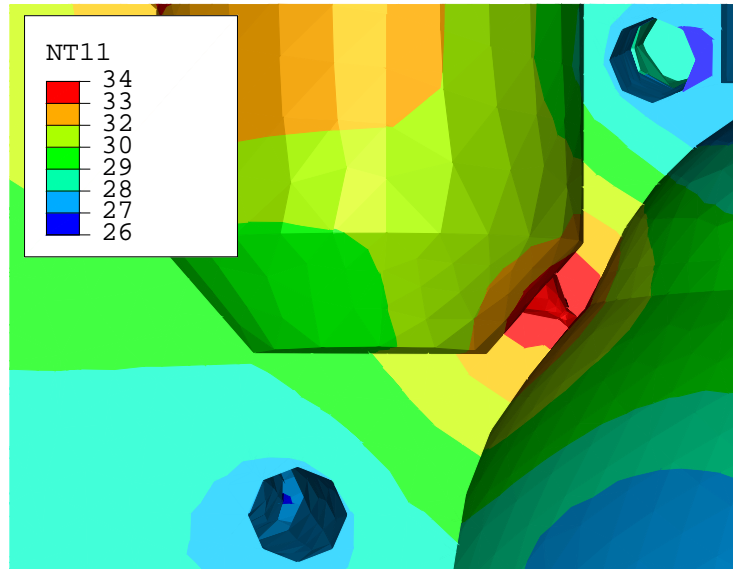


Figure 6.1: Section cut of the cavity tool in the injection area.

The temperature in the cavity tool is important for the understanding of the thermodynamics, but it is the temperature in and on the top that decides when the polymer top can be ejected from the cavity tool. Figure 6.2 shows the temperature on the outer surface of the polymer top and on the cavity surface of the cavity tool in the injection area, i.e. the warmest zone. The difference between the warmest and coolest zone is  $\sim 2\text{ }^\circ\text{C}$  on the polymer top in contact with the cavity tool.

A steady temperature level is reached after only 2 cycles and the top have a final temperature of  $107\text{ }^\circ\text{C}$  at the end of a cycle, which could be compared to HDPE's melting temperature of  $\sim 130\text{ }^\circ\text{C}$ . In Figure 6.3 the 10th and last cycle is enlarged and a center and inner surface node from the injection area of the polymer top is added to show where the final temperature is highest. The center node is placed between the inner and outer surface node, cf. Figure 5.1.

In Figure 6.3, the simulated steps can be interpreted from the different curve derivatives which depend on the change of heat transfer coefficient in the cavity chamber during the cycle. An increased heat transfer coefficient increases the temperature derivatives and vice versa. Moreover, a significant reduction of the derivative can be seen in the curvatures when the nodes reach temperatures around  $135\text{ }^\circ\text{C}$ , this is because of the peak in the specific heat for the polymer, i.e. the phase when the polymer is solidified. The highest final temperature is seen on the outer surface on the polymer, this is because the outer surface is reheated again from the center of the polymer top when the cavity tool is removed. A comparison can be made with a boiled egg placed in cold water to cool down. The temperature seems

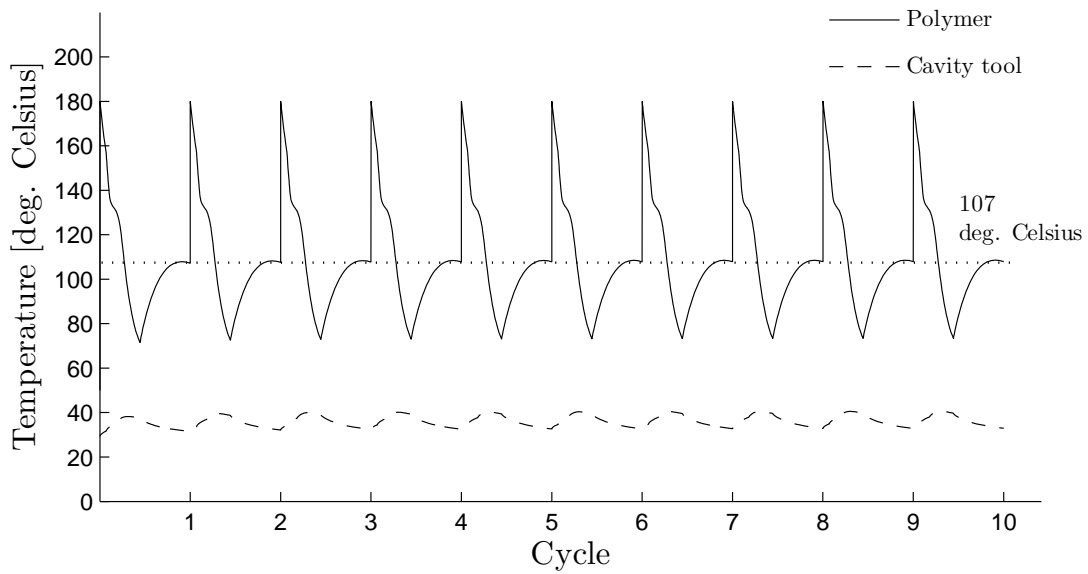


Figure 6.2: Temperature in the injection zone at the polymer top and cavity tool, made of aluminium, during ten cycles.

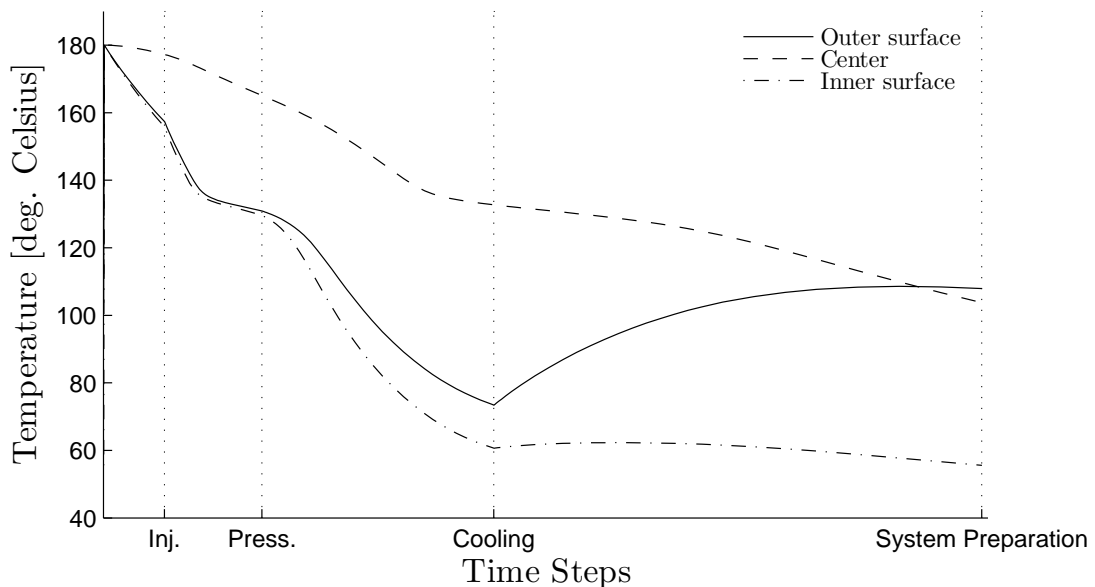


Figure 6.3: The temperature for three nodes, outer surface, inner surface and in the center at the injection zone on the polymer are shown over the last cycle.

cold if a hand is placed around the egg, the heat from the egg is transported to the water with relative high heat transfer coefficient. This means that the water cools the surface of the egg faster than the egg can transport heat from its hot core to the surface. If the egg

is removed from the water to the air, resulting in a lower heat transfer coefficient, the hot core heats the surface of the egg and it feels hot. The inner surface of the polymer top is also reheated, although not as much as the outer surface, and the heat transfer coefficient is reduced to  $1600 \text{ W/m}^2\text{K}$ . The heat transfer coefficient is the same for the inner and outer polymer surface in the injection, pressing and cooling step, although the two surfaces show a difference in temperature. This depends on the difference in temperature of the cavity tool and the core tool. While the core tool is assumed to have a constant temperature of  $25 \text{ }^\circ\text{C}$  the cavity tool is heated.

## 6.2 FE Simulation Using Steel as Tool Material

This section demonstrates the convenience of simulating the IM process in a computer. The cavity tool is originally made out of aluminium, but how does a change in material to steel effect the IM process? The thermal material properties of steel have negative effects compared to aluminium regarding cooling of the polymer top, shown in section 4.2. Other material properties show that steel are more suited as cavity tool material, but will a change result in a increased cycle time? Material data from Table 6.1 was implemented in the FE model and a simulation of 10 cycles with the new settings was made.

Table 6.1: Thermal conductivity, density and specific heat for steel.

|       | $\lambda$<br>[W/mK] | $\rho$<br>[kg/m <sup>3</sup> ] | $C_p$<br>[J/kgK] |
|-------|---------------------|--------------------------------|------------------|
| Steel | 40                  | 7850                           | 565              |

The number of cycles required to obtain a steady temperature level are not as rapid as in previous simulation results, when using a cavity tool made out of aluminium, cf. Figure 6.4. The final temperature does not stabilize until approximately 10 cycles have been completed. A comparison of the last cycle on the temperature at the outer surface with the results when using aluminium as cavity tool material shows that there is an increase in temperature when using steel as cavity tool material, cf. Figure 6.5.

The end of the cycle in Figure 6.5 shows that there is a  $7 \text{ }^\circ\text{C}$  difference in the final temperature on the polymer depending on what material is used for the cavity tool. The  $114 \text{ }^\circ\text{C}$  on the polymer surface is lower than the melting temperature and steel could therefore be used as cavity tool material with a cycle time of 1.44 seconds.

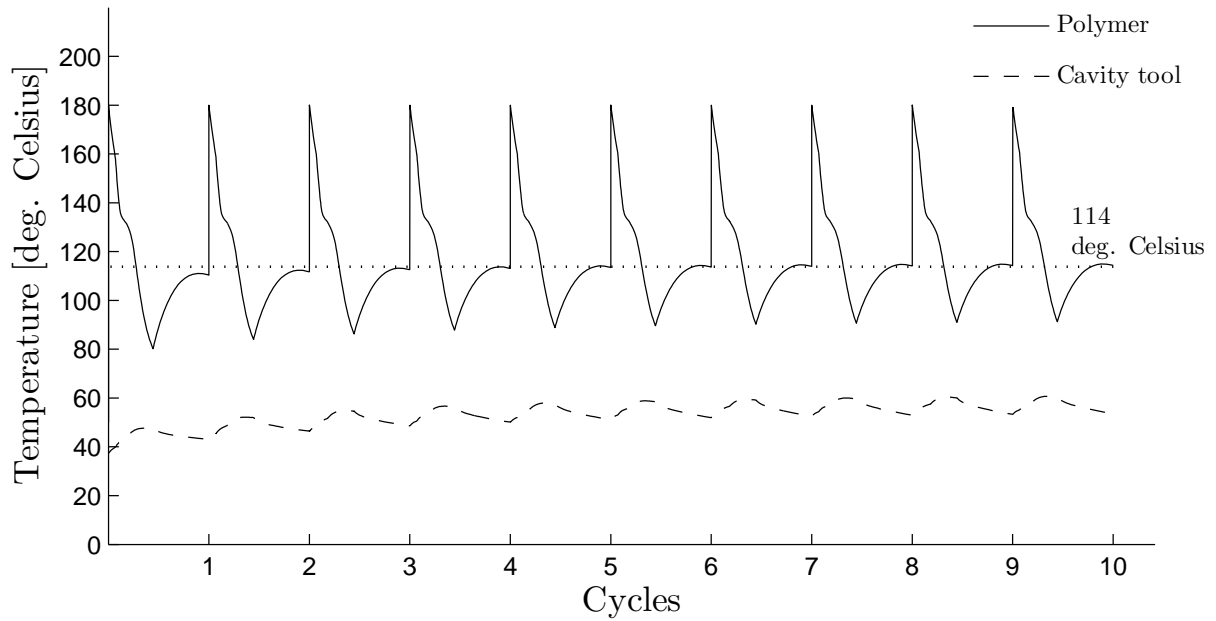


Figure 6.4: Temperature in the injection zone at the outer surface of the polymer top and at the cavity surface on the cavity tool during ten cycles, using steel as cavity tool material.

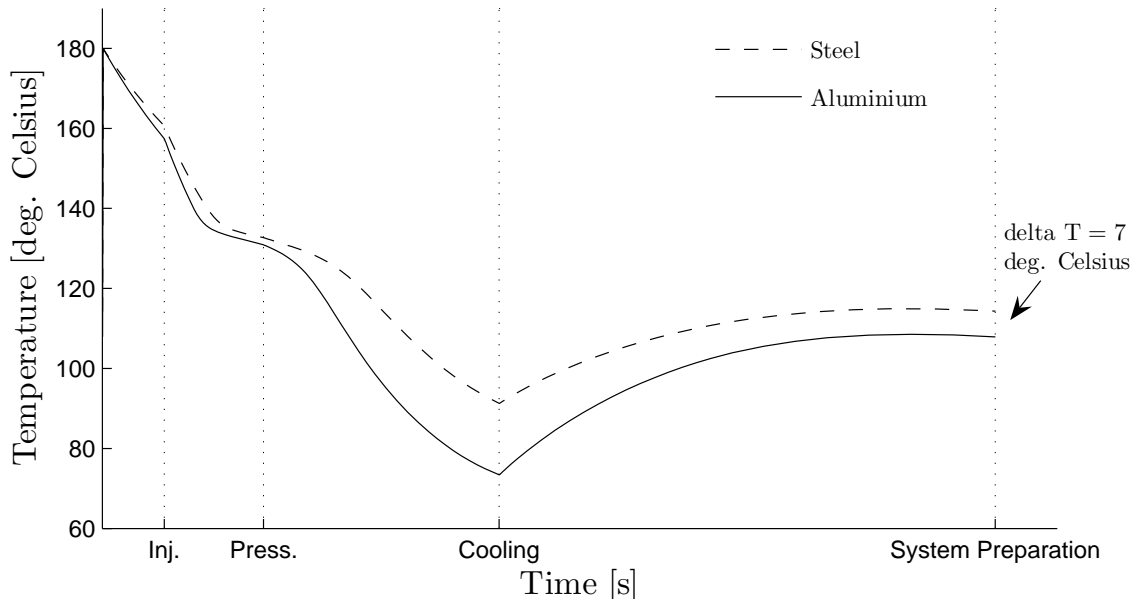


Figure 6.5: The temperature of the polymer top's outer surface in the injection zone when using either steel or aluminium as cavity tool material.

### 6.3 Energy Balance

If the cavity tool is considered as a closed system an energy balance can be calculated. The hot runners and the polymer top supplies energy to the cavity tool and the cooling channels transport energy out from the cavity tool. If the system is at steady state the sum of the energy balance equation will be equal to zero at the end of a cycle

$$Q_{Top} + Q_{Hot\ runner} - Q_{Cooling\ channel} = 0$$

where  $Q_{Top}$  denotes the energy from the top,  $Q_{Hot\ runner}$  the energy from the hot runners and  $Q_{Cooling\ channel}$  the energy removed by the cooling channels. Using the simulation with aluminium as cavity tool an energy balance for the last step is calculated. When a contact is specified in ABAQUS, the command HFLA (Heat FLux vector multiplied by the Area) enables the possibility to store the heat transported through the surfaces at every time increment. Surfaces with no contact, as the cooling channel's, could also be pre-selected with the command SOH to store the heat transportation. Using this for the hot runners, polymer top and cooling channels an energy balance is obtained, cf. Figure 6.6.

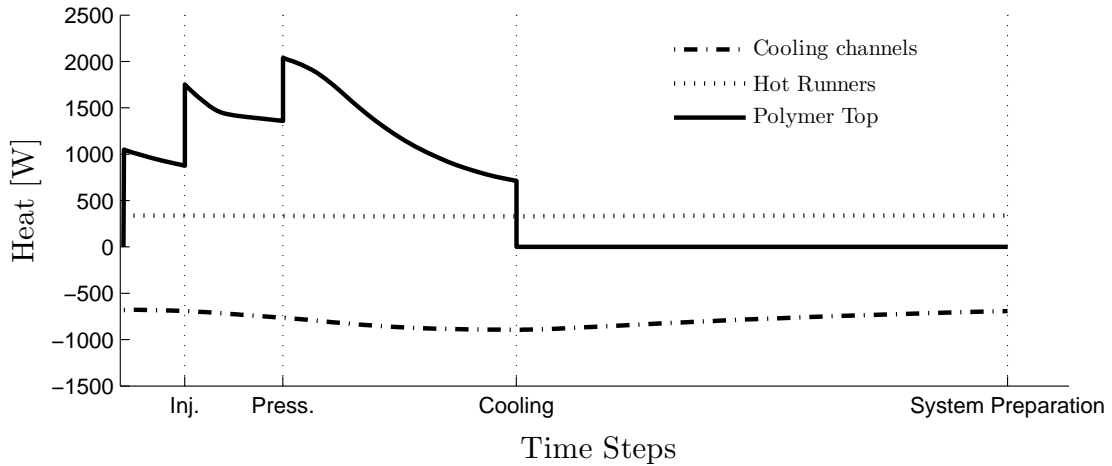


Figure 6.6: Power graph for the 10th cycle when using Aluminium as cavity tool material.

A heat rate of approximately 340 W from the hot runners is continuously applied to the cavity tool during the cycle. The polymer top delivers between 700 to 2000 W and 680 to 900 W is removed by the cooling channels. The heat applied from the hot runners and the heat removed by the cooling channels is almost linear. The heat from the polymer top reflects the steps in the cycle, an increase in heat transfer coefficient increases the heat applied to the tool. Using the graphs in Figure 6.6 and integrating over time,  $Q_{Top}$ ,  $Q_{Hotrunner}$  and  $Q_{Coolingchannel}$  could be obtained.



Table 6.2: Energy balance of the cavity tool.

|            | Energy [J] |
|------------|------------|
| $Q_{Top}$  | 814        |
| $Q_{HR}$   | 482        |
| $Q_{C.Ch}$ | -1133      |
| Total      | 163        |

As seen in Table 6.2 the energy balance does not equals zero, this even though a steady temperature level is reached in the cavity chamber area. The cavity tool weigh 2.5 kg and the specific heat for Aluminium is 890 J/kgK. Using this, the increased temperature of the cavity tool could be calculated. The results show an average temperature increase of 0.07 °C.



# Chapter 7

## Improvement Proposals

Having seen the results from the original design of the cavity tool improvement proposals was prepared. A trial to eliminate the negative factors from the original cavity tool design, and thereby receive a lower temperature at the cavity chamber, was made. This will result in the possibility to cool the polymer top more efficient and enable an earlier ejection from the cavity tool, i.e. a reduction of cycle time.

### 7.1 Minimization of Heat Input to the Cavity Tool

A negative factor is the heat flowing out from the hot runners in to the cavity tool. This gives the consequence that more heat has to be generated in the hot runners to keep the melted polymer temperature at an acceptable level, i.e.  $\sim 200$  °C. As seen in the energy balance the cavity tool is applied with 482 J from the hot runners during a cycle. The improvement proposal aims to reduce the heat from the hot runners applied to the cavity tool.

By increasing the diameter of the drilled holes in the cavity tool, for the hot runners, enough space will be created to enable an assembly of a thin walled cylinder with four flanges, cf. Figure 7.1.

The cylinder is made out of stainless steel, resulting in a high temperature gradient within the material because of the low thermal conductivity, shown in section 4.2. The only contact between the cylinder and the cavity tool is via the four flanges. Between the flanges air interacts, which have a thermal conductivity of  $\sim 0.025$  W/mK. An assumption is therefore made that no heat is transported through the air. This modification will help to isolate the upper part of the hot runner.

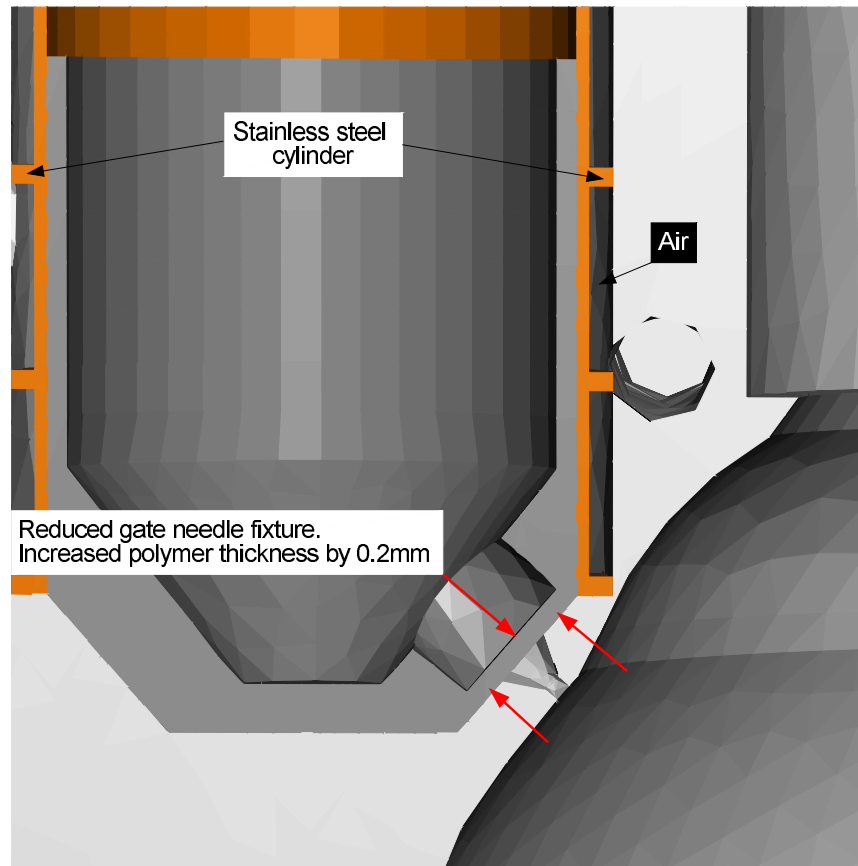


Figure 7.1: A section cut of the tool with the isolating (highlighted) cylinder implemented and the thickened polymer at the injection zone.

Table 7.1: Material data for stainless steel.

|                 | $\lambda$<br>[W/mK] | $\rho$<br>[kg/m <sup>3</sup> ] | $C_p$<br>[J/kgK] |
|-----------------|---------------------|--------------------------------|------------------|
| Stainless Steel | 14                  | 8000                           | 440              |

For the lower conical shaped part a small change in dimension on the fixture, the nut that stabilize the gate needle, will reduce the heat flow. As mentioned earlier in this report the polymer is a good isolator. Therefore, by making the layer of melted polymer between the hot runner and the cavity chamber slightly thicker, 0.2 mm, a noticeable reduction of the heat flow from the hot runner will hopefully be seen. Simulations with the improvement proposal is made using the same coolant temperature, coolant flow and hot runner temperature as previous. Figure 7.2 shows the temperature in the cavity chamber for the previous and the improved design.

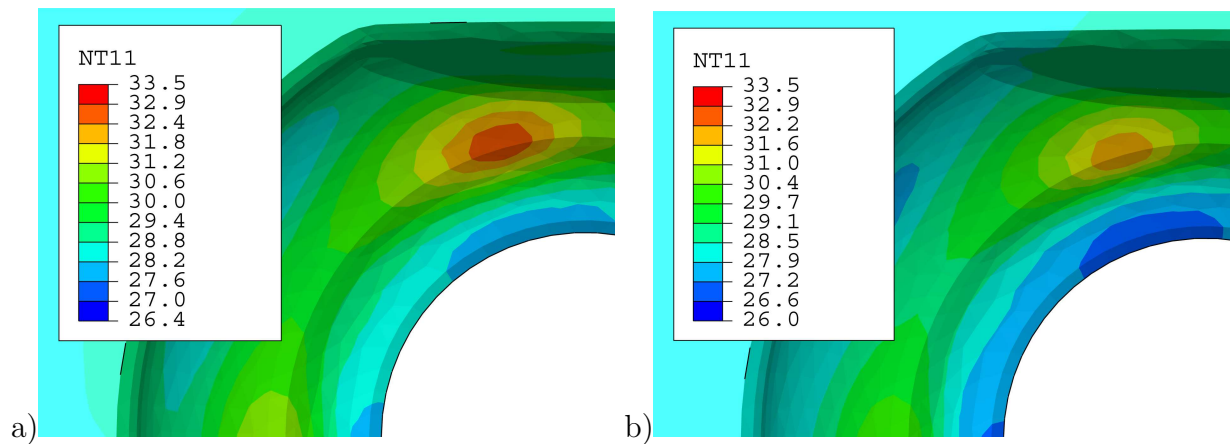


Figure 7.2: Temperature in the cavity tool made of aluminium using a) original design. b) improved design.

The temperature level is lower for the improved design in the cavity chamber, but the difference is small. The temperature on the polymer top was compared for the two designs and a negligible change could be seen. However, the heat from the hot runners was reduced with 50 %, from  $\sim 340$  W to  $\sim 170$  W but this reduction did not affect the cooling of the polymer top.

## 7.2 Coolant Temperature

The improved design resulted in a negligible temperature improvement on the polymer top. However, the energy loss from the hot runners to the tool was reduced with 50 %, this when using a coolant temperature of  $25$  °C. This render the possibility to use a coolant with a temperature considerably lower than simulated temperatures without any risk to exceed the hot runners maximum power capacity of 1000 W. Unfortunately, if temperatures under  $25$  °C is used there is a risk for condensation in the IM surroundings which is not acceptable in an aseptic point of view. If the aseptic subject is solved or disregarded the improved design enables for a lower coolant temperature which reduces the cycle time. Figure 7.3 shows how the temperature of the cavity and core surface affect the outer surface temperature of the polymer top.

A small piece have been cut out from the FE model, same as Figure 4.12 and the diverse temperatures in Figure 7.3 represent the initial cavity tool temperature. A  $20$  °C decrease in temperature of the cavity and core tool reduced the final temperature of the top with  $11$  °C. Remark that  $10$ ,  $20$ ,  $30$  °C is the temperature of the tool, the temperature level for the coolant has to be lower.

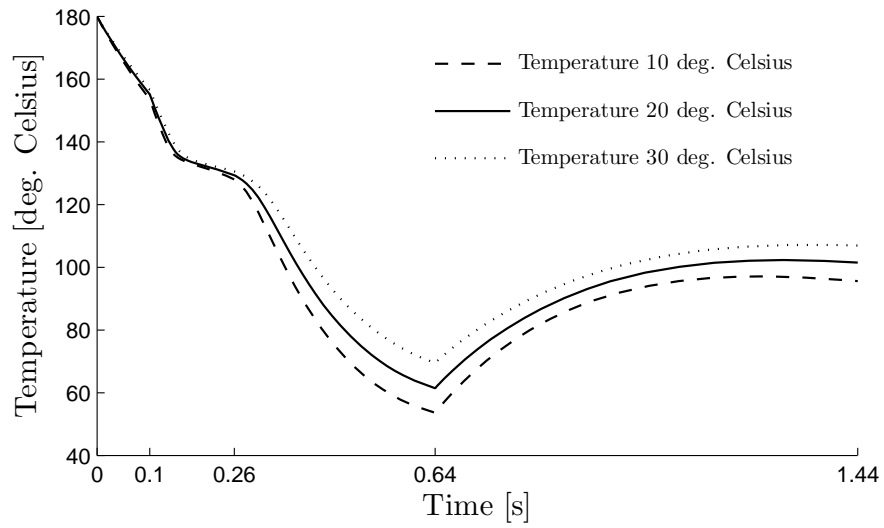


Figure 7.3: The temperature, at the outer surface of a small piece of the polymer top, using different tool temperatures.

# Chapter 8

## Discussion

During the work of creating a FE model a lot of effort was spend on the research of material data, since this constitute an important part of the modelling. Reliable temperature dependent data on specific heat for the polymer, HDPE, was of importance because of the discontinuity around freezing temperature where the specific heat peaks at values significantly higher than during the rest of the temperatures. Other material data, density and thermal conductivity, in the diverse materials was not significantly temperature dependent and are therefore only as detailed as the time frame of this master thesis allowed. An assessment made is that good quality data for this work has been gathered and should therefore give an accurate description of the materials behaviour.

There have been some approximations on the geometry for the analysed parts, mainly to facilitate the work of meshing the parts. The only region where the geometry approximation can be discussed is on the top. A top is created with a homogenous thickness of 0.7 mm which distinguish from the real top that have a various thickness between 0.6-0.8 mm. Because of the low thermal conductivity in the polymer this could have some influence on the results and should therefore, if possible, be modelled as precise as feasible.

In this model the core tool and the actual hot runners have only been described as conditions. These assumptions are made to save calculation time. The actual hot runners are automatically controlled to supply a constant temperature and the core tool is cooled between every IM cycle. This results in a fairly constant thermal state which is described with a boundary condition and film condition.

A time chart was created describing all the events occurring during a production cycle. Because of the complexity to model a flow in ABAQUS the FE model includes only one geometry of the polymer top, this disable the ability to accurately reproduce the event of the injection and pressing step. Trying to compensate for this flaw values on the heat transfer coefficient was set in order to reduce the heat flow to a more likely level. A statistical study, DOE, was made where it is presented that the injection and pressing step only has a modest influence and that it is the cooling and system preparation step that is

important to reproduce accurately. These results suggest that the approximation done in the injection and pressing step will not have any severe influence on the results.

Two articles were used to set a value for the heat transfer coefficient in the cooling step. The first article stated a value for the heat transfer coefficient and the second article concluded that the coefficient is constant during the cooling step. The values for the heat transfer coefficient during the other steps in the cycle were decided together with expertise from Tetra Pak Packaging Solutions AB. Since the influence from the injection and pressing step is small, shown in the design of experiments, and that it is likely that the value for the heat transfer coefficient in the cooling step is correct, the system preparation step is the only uncertain factor. The value on the heat transfer coefficient in the system preparation step, depends on whether the shrinkage of the polymer preserves the contact pressure against the core tool or not, when the cavity tool is removed.

One question that was brought up is, if it is necessary to make a simulation of the whole cavity tool and it's interacting parts. A tremendous advantage will be made in calculation time if it is possible to focus on only the critical area in this tool and set boundary conditions that represent the surroundings from the whole FE model. Successful attempts were made where the small model delivered result almost identical to the whole FE model's results. However, this is for simulation during one cycle only. Trying to simulate a continuous production can be difficult since it is hard to predict how the surroundings is affected in the long term.

## 8.1 Conclusion

The main objective of this thesis was to investigate if a FE model can be used to simulate the thermodynamics in an IM process and to obtain knowledge of how constitutive laws and material data for this application should be defined to receive accurate results. An experiment conducted on a test rig was compared with results from the FE simulation made in ABAQUS. The outcome of this study showed that the thermodynamics within the core tool can be simulated delivering results with accuracy of 1-3 °C. An extensive part of this report describes in detail which input data is needed and how to perform a thermal analysis on an arbitrary IM tool, for future projects at Tetra Pak. An extension of this work was, for natural reasons, to evaluate the results and highlight the critical areas in the simulated tool for further development.

The polymer can not be ejected from the cavity tool until a desired temperature is reached. The temperature of the top therefore decides the cooling time needed before ejection. Results from the simulation showed that the injection zones, both on the cavity tool and the polymer top's outer surface, reaches highest temperatures and is hence the most critical area in the design. The highest final temperature in the polymer top is 107 °C when using aluminium as cavity tool material, this can be compared with ~130 °C which is the polymers



melting temperature. If a cavity tool made of steel is used an increase of 7 °C is received on the polymer top. From a thermal perspective aluminium is clearly favourable but there are often mechanical characteristic that forces the use of steel, usually because an aluminium tool wear to quickly. This possibility, to change tool material, is a demonstration of the advantages in using FEM instead of having to manufacture the tools which is very costly. A study of the cavity tool made out of aluminium shows that the most critical areas have a temperature of 34 °C which is 9 °C above the coolants temperature. A constant flow of 340 W is flowing from the hot runners into the cavity tool during the cycle which is almost 40 % of the total heat input to the cavity tool.

A proposal of a conceivable design was presented where the hot runners was designed with a cylinder, made out of stainless steel, with flanges to create an isolating layer of air. Also, a change in the design of the stabilizing fixture for the gate needle was made. This is made to enhance the thickness of the isolating polymer in the most critical area of the tool. The outcome of this design showed that the heat loss from the hot runners into the cavity tool was reduced with 50 % and a temperature drop on the cavity tools surface in the cavity chamber with 2 °C. These improvements on the cavity tool result in an insignificant temperature drop on the polymer top.

From these results a conclusion is that the design of the cooling system in the cavity tool today is not limiting the cooling time. The area where the highest temperature is present in the cavity tool is only 10 °C above the coolant's temperature and even if it is designed perfectly the cavity tool can not reach temperatures lower than the coolant temperature of 25 °C. A temperature in the cavity tool of 25 °C will only decrease the highest final temperature of the top with about 4 °C. If the restriction of a minimum temperature of the coolant, because of condensation, is revoked, this would render the possibility to lower the coolants temperature, without any risk to exceed the hot runners capacity, and thereby reduce the cooling time. Another problem is the heat in the center (core) of the polymer thickness which is difficult to cool, the center stays isolated by the polymer surface resulting in longer cooling time.

## 8.2 Further Work

The lowest coolant temperature allowed within the IM process is 25 °C. This thesis shows that the coolant temperature have significant effect on the temperature of the polymer top. It is therefore of further interest and work to enable the possibility to use a coolant temperature lower than 25 °C without effecting the aseptic criteria.

The polymer top have a thermal conductivity of 0.32 W/mK, this relatively low number prevents a fast heat removal, especially in the center of the polymer top's thickness. An increase of the thermal conductivity would enable a more efficient cooling. The thickness of the polymer top is also a factor that effect the cooling, a thick top increases the cooling

time due to the low thermal conductivity and more mass, i.e. more energy, needs to be removed. It is therefore of interest to investigate if the thermal conductivity could be increased, e.g. with a compound, and analyse if a reduction in the thickness of the polymer top could be made.

The heat transfer coefficient in the system preparation step includes an uncertainty. Experiments, in whether the shrinkage of the polymer preserves a high contact pressure against the core tool, could give more knowledge and input to the FE model.

# Bibliography

- [1] Becker J, Berggren K, Nilsson L-Å, Strömvall H-E. *Formsprutningsteknik*. Stockholm: YFIND; 2000.
- [2] Tetra Pak [homepage on the Internet]. Product information Tetra Top [cited 2007 Jan 12]. Available from: <http://www.tetrapak.com/>.
- [3] *ABAQUS Inc.* part of Dassault Systmes Available from: <http://www.abaqus.com/>.
- [4] Georgia Institute of Technology [homepage on the Internet]. [cited 2007 Feb 25] Available from: <http://www.me.gatech.edu/jonathan.colton/me4793/injection.pdf>
- [5] Sun YF, Lee KS, Nee AYC. *Design and FEM analysis of the milled groove insert method for cooling of plastic injection moulds*. Int J Adv Manuf Technol. 2004 May 5;24:715-726
- [6] Saabye Ottosen N, Petersson H. *Introduction to the FINITE ELEMENT METHOD*. Prentice Hall Europe; 1992.
- [7] Saabye Ottosen N, Ristinmaa M. *The Mechanics of Constitutive Modelling: Numerical and thermodynamical topics*. vol. 2. Lund: Div. of Solid Mechanics Lund University; 1999.
- [8] Jean Baptise Fourier. *Thorie analytique de la chaleur*. [cited 2007 Jan 23]. Available from: <http://www.lub.lu.se/>.
- [9] Smith EH. *Mechanical Engineer's Reference Book*. [database on the Internet] 12th ed. Elsevier: Knovel. c2003 [cited 2006 Dec 20]. <http://www.knovel.com/knovel2/Toc.jsp?BookID=676&VerticalID=0>.
- [10] Ekroth I, Granryd E. *Tillämpad Termodynamik* [Applied Thermodynamics]. Stockholm: Royal Institute of Technology; 2005.
- [11] Sundén B. *Värmeöverföring* [Heat Transfer]. Lund: Studentlitteratur; 2006.
- [12] Alberto Naranjo C, Maria del Pilar Noriega E, Juan Diego Sierra M, Juan Rodrigo Sanz *Injection Molding Processing Data*. Munich: Carl Hanser Verlag; 2001

- [13] Tetra Pak Packaging Solutions AB. Material Data from the department of PM - Material Analysis. Johan Persson. Lab Scientist: 2007 Jan 11.
- [14] Uddeholm [homepage on the Internet]. Thermal conductivity and density for ALUMEC [cited 2007 Feb 07]. Available from: <http://www.uddeholm.se/>.
- [15] *ABAQUS Theory Manual*. v6.5. USA: ABAQUS; 2004.
- [16] *ABAQUS Analysis User's Manual*. v6.5-1. Section 21.2.4
- [17] Kamal MR, Mutel AT, Salloum G, Garcia-Rjon A. *Heat Transfer Measurement at the Mold Surface During Injection Molding of Thermoplastic Melts*. McGill University and National Research Council Canada. Antec 91:483-486
- [18] Bendada A, Derdouri A, Lamontagne M, Simard Y. *Analysis of thermal contact resistance between polymer and mold in injection molding*. National Research Council Canada. Applied Thermal Engineering 24 (2004):2029-2040
- [19] Minitab release 14 for Windows [homepage on the Internet]. [cited 2007 Feb12]. Available from: <http://www.minitab.com/>.
- [20] European co-operation for Accreditation [homepage on theInternet]. [cited 2007 Feb 25] Available from: <http://www.european-accreditation.org/n1/doc/EA-4-02.pdf>

# Appendix A

## ABAQUS/Standard Input File

```
**
** FE Simulation of TETRA PAK's INJECTION COMPRESSING MOULDING
**
** written by RIKARD JOHANSSON and Daniel Konijnendijk
**
*Heading
** Job name: FE_Model Model name: Version_11
*Preprint, echo=NO, model=NO, history=NO, contact=NO
**
**-----
***   R E G U L A T E D   P A R A M E T E R S
**-----
*PARAMETER
ch_factor = 1
**-----
*****   CAVITY   *****
**-----
injection = 800*ch_factor
pressing = 1600*ch_factor
cooling = 2400*ch_factor
system_prep = 1600*ch_factor
**-----
*****   COOLING CHANNELS   *****
**-----
cool2=25632*ch_factor
cool3=37610*ch_factor
cool4=36696*ch_factor
cool5=36696*ch_factor
cool6=37443*ch_factor
cool7=28221*ch_factor
cool8=26022*ch_factor
cool9=25310*ch_factor
cool10=25370*ch_factor
cool11=25310*ch_factor
```

APPENDIX A. ABAQUS/STANDARD INPUT FILE

---

```

cool12=25370*ch_factor
cool13=29900*ch_factor
cool14=29738*ch_factor
low_flow=5000*ch_factor
**-----
*****   Hot Runner   *****
**-----
hot_runner = 2400
**
**-----
***           P A R T   H O T   R U N N E R   1
**-----
*Part, name=HDPE_Hot_Runner_1
*Node
    1, -0.021106001, -0.0366002284, 0.0449000001
    ., ., ., .
    ., ., ., .
    ., ., ., .
    1773, -0.00291182962, -0.0354309566, 0.0385661088
*Element, type=DC3D8
    1, 58, 27, 28, 57, 547, 436, 437, 546
    ., ., ., ., ., ., ., ., .
    ., ., ., ., ., ., ., ., .
    ., ., ., ., ., ., ., ., .
    272, 422, 753, 754, 421, 169, 116, 117, 168
*Element, type=DC3D4
    273, 1319, 1320, 1321, 857
    ., ., ., ., .
    ., ., ., ., .
    ., ., ., ., .
    5210, 1712, 889, 1713, 968
*Nset, nset=Temp_HR1
    1, 4, . . .
*Nset, nset=Watt_HR1
    2, 3, . . .
** Section: HDPE_section
*Solid Section, elset=_HDPE_Hot_Runner_1, material=HDPE
1.,
*End Part
**
**-----
***           P A R T   H O T   R U N N E R   2
**-----
*Part, name=HDPE_Hot_Runner_2
. . .
**-----
***           P A R T   H O T   R U N N E R   3
**-----
*Part, name=HDPE_Hot_Runner_3
. . .
**-----

```

APPENDIX A. ABAQUS/STANDARD INPUT FILE

---

```

***          P A R T   H O T   R U N N E R   4
**-----
*Part, name=HDPE_Hot_Runner_4
. . .
**-----
***          H D P E   T O P
**-----
*Part, name=HDPE_Top
*Node
    2535, -0.0207599998,  8.26539601e-11, 0.0492536649
        .,              .,              .,              .
        .,              .,              .,              .
        .,              .,              .,              .
    10136, 0.0164417755,  0.0356772803, 0.0132683339
*Element, type=DC3D8
2443, 2535, 2643, 3188, 2562, 5069, 5177, 5722, 5096
    ., ., ., ., ., ., ., ., .
    ., ., ., ., ., ., ., ., .
    ., ., ., ., ., ., ., ., .
7326, 7602, 7538, 5705, 5704,10136, 10072, 8239, 8238
*Elset, elset=Top_temp, generate
    2443, 7326, 1
*Elset, elset=Injection, generate
    2443, 7326, 1
*Surface, type=ELEMENT, name=OffsetElements-Inner_Tool
*Surface, type=ELEMENT, name=Cavity_Surface_1
.
.
.
*Surface, type=ELEMENT, name=Cavity_Surface_40
** Region: (HDPE_section:Picked)
*Elset, elset=_HDPE_Top, internal, generate
    2443, 7326, 1
** Section: HDPE_section
*Solid Section, elset=_HDPE_Top, material=HDPE
1.,
*End Part
**
**-----
***          C A V I T Y   T O O L
**-----
*Part, name=cavity_tool
*Node
    1, 0.0179164279, 0.0624820106, 0.
        .,              .,              .,              .
        .,              .,              .,              .
        .,              .,              .,              .
    45831, -0.0103358598, -0.0529843085, 0.00464495085
*Element, type=DC3D8
    1, 535, 536, 3618, 3610, 3629, 3630, 14106, 14098
        ., ., ., ., ., ., ., ., .

```

APPENDIX A. ABAQUS/STANDARD INPUT FILE

---

```

      .,      .,      .,      .,      .,      .,      .,      .,      .
      .,      .,      .,      .,      .,      .,      .,      .,      .
2280, 15520, 15536, 15521, 15517, 3612, 3628, 3613, 3609
*Element, type=DC3D4
  2281, 15537, 15538, 15539, 15540
      .,      .,      .,      .,      .
      .,      .,      .,      .,      .
      .,      .,      .,      .,      .
226771, 39439, 42893, 44189, 45674
*Surface, type=ELEMENT, name=Section_2
.
.
.
*Surface, type=ELEMENT, name=Section_14
*Surface, type=ELEMENT, name=Section_Low_Flow
*Surface, type=ELEMENT, name=H_1
.
.
.
*Surface, type=ELEMENT, name=H_4
*Surface, type=ELEMENT, name=Cavity_Tool_Cavity_Surface
.
.
.
*Surface, type=ELEMENT, name=Cavity_Tool_Cavity_Surface_40
** Region: (Aluminium_section:Picked)
*Elset, elset=cavity_tool, internal, generate
  1, 226771, 1
** Section: Aluminium_section
*Solid Section, elset=cavity_tool, material=Aluminium
1.,
*End Part
**
**-----
***                A S S E M B L Y
**-----
*Assembly, name=Assembly
**
*Instance, name=HDPE_Hot_Runner_1-1, part=HDPE_Hot_Runner_1
*End Instance
**
*Instance, name=HDPE_Hot_Runner_2-1, part=HDPE_Hot_Runner_2
*End Instance
**
*Instance, name=HDPE_Hot_Runner_3-1, part=HDPE_Hot_Runner_3
*End Instance
**
*Instance, name=HDPE_Hot_Runner_4-1, part=HDPE_Hot_Runner_4
*End Instance
**
*Instance, name=Cavity_tool-1, part=Cavity_tool

```



## APPENDIX A. ABAQUS/STANDARD INPUT FILE

---

```
*End Instance
**
*Instance, name=HDPE_Top-1, part=HDPE_Top
*End Instance
**
*End Assembly
**
**-----
***                M A T E R I A L S
**-----
*Material, name=Aluminium
*Conductivity
165.,
*Density
2830.,
*Specific Heat
  840.73, 25.0574
  840.872, 25.1255
  841.002, 25.1909
    ., .
    ., .
    ., .
  946.504, 100.029
*Material, name=HDPE
*Conductivity
  0.32,
*Density
1050.,
*Specific Heat
  1801., 50.
  1800., 51.
  1818., 52.
    ., .
    ., .
    ., .
  2287.,200.
**
**-----
***  I N T E R A C T I O N    P R O P E R T I E S
**-----
*Surface Interaction, name="Contact Hotrunners"
1.,
*Gap Conductance
<hot_runner>, 0.
<hot_runner>, 5.
  0.,10.
*Surface Interaction, name=Cooling
1.,
*Gap Conductance
<cooling>, 0.
<cooling>, 0.005
```

APPENDIX A. ABAQUS/STANDARD INPUT FILE

---

```

    0., 0.01
*Surface Interaction, name=Injection
1.,
*Gap Conductance
<injection>, 0.
<injection>, 0.005
    0., 0.01
*Surface Interaction, name=Pressing
1.,
*Gap Conductance
<pressing>, 0.
<pressing>, 0.005
    0., 0.01
*Surface Interaction, name=System_Prep
1.,
*Gap Conductance
0., 0.
0., 0.01
**
**-----
***          P R E D E F I N E D      F I E L D S
**-----
** Name: Initial_Temp   Type: Temperature
*Initial Conditions, type=TEMPERATURE
Cavity_Tool_and_HR, 50.
** Name: Top_temp      Type: Temperature
*Initial Conditions, type=TEMPERATURE
Top, 50.
**
**-----
***          I N T E R A C T I O N S
**-----
** Interaction: Cavity_Injection
*Contact Pair, interaction=Injection
HDPE_Top-1.Cavity_Surface_1, Cavity_tool-1.Cavity_Tool_Cavity_Surface
** Interaction: Cavity_Pressing
*Contact Pair, interaction=Pressing
HDPE_Top-1.Cavity_Surface_2, Cavity_tool-1.Cavity_Tool_Cavity_Surface_2
** Interaction: Cavity_Cooling
*Contact Pair, interaction=Cooling
HDPE_Top-1.Cavity_Surface_3, Cavity_tool-1.Cavity_Tool_Cavity_Surface_3
** Interaction: Cavity_System_Prep
*Contact Pair, interaction=System_Prep
HDPE_Top-1.Cavity_Surface_4, Cavity_tool-1.Cavity_Tool_Cavity_Surface_4
.
.
.
** Interaction: Cavity_System_Prep
*Contact Pair, interaction=System_Prep
HDPE_Top-1.Cavity_Surface_40, Cavity_tool-1.Cavity_Tool_Cavity_Surface_40
**

```

## APPENDIX A. ABAQUS/STANDARD INPUT FILE

---

```
** Interaction: H1_HR1
*Contact Pair, interaction="Contact Hotrunners", small sliding, type=SURFACE TO SURFACE
HDPE_Hot_Runner_1-1.HR_1, Cavity_tool-1.H_1
** Interaction: H2_HR2
*Contact Pair, interaction="Contact Hotrunners", small sliding, type=SURFACE TO SURFACE
HDPE_Hot_Runner_2-1.HR_2, Cavity_tool-1.H_2
** Interaction: H3_HR3
*Contact Pair, interaction="Contact Hotrunners", small sliding, type=SURFACE TO SURFACE
HDPE_Hot_Runner_3-1.HR_3, Cavity_tool-1.H_3
** Interaction: H4_HR4
*Contact Pair, interaction="Contact Hotrunners", small sliding, type=SURFACE TO SURFACE
HDPE_Hot_Runner_4-1.HR_4, Cavity_tool-1.H_4
**
**
** -----
**
**                W A R M        U P
**
** -----
**
**Step, name="Warm_up", amplitude=RAMP, inc=100000
*Heat Transfer, steady state, deltmx=0.
0.0001, 1., 1e-07, 1.,
**
** BOUNDARY CONDITIONS
**
** Name: Hot_Runner_Temp_1 Type: Temperature
*Boundary
HDPE_Hot_Runner_1-1.Temp_HR1, 11, 11, 200.
** Name: Hot_Runner_Temp_2 Type: Temperature
*Boundary
HDPE_Hot_Runner_2-1.Temp_HR2, 11, 11, 200.
** Name: Hot_Runner_Temp_3 Type: Temperature
*Boundary
HDPE_Hot_Runner_3-1.Temp_HR3, 11, 11, 200.
** Name: Hot_Runner_Temp_4 Type: Temperature
*Boundary
HDPE_Hot_Runner_4-1.Temp_HR4, 11, 11, 200.
**
** INTERACTIONS
**
** Interaction: Cavity_Injection
*Model Change, type=CONTACT PAIR, remove
HDPE_Top-1.Cavity_Surface_1, Cavity_tool-1.Cavity_Tool_Cavity_Surface
** Interaction: Cavity_Pressing
*Model Change, type=CONTACT PAIR, remove
HDPE_Top-1.Cavity_Surface_2, Cavity_tool-1.Cavity_Tool_Cavity_Surface_2
** Interaction: Cavity_Cooling
*Model Change, type=CONTACT PAIR, remove
HDPE_Top-1.Cavity_Surface_3, Cavity_tool-1.Cavity_Tool_Cavity_Surface_3
** Interaction: Cavity_System_Prep
```

APPENDIX A. ABAQUS/STANDARD INPUT FILE

---

```

*Model Change, type=CONTACT PAIR, remove
HDPE_Top-1.Cavity_Surface_4, Cavity_tool-1.Cavity_Tool_Cavity_Surface_4
.
.
.
** Interaction: Cavity_System_Prep
*Model Change, type=CONTACT PAIR, remove
HDPE_Top-1.Cavity_Surface_40, Cavity_tool-1.Cavity_Tool_Cavity_Surface_40
**
** Interaction: Cooling chanel_Low flow
*Sfilm
Cavity_tool-1.Low_Flow, F, 25., <low_flow>
** Interaction: Cooling chanel_S2
*Sfilm
Cavity_tool-1.Section_2, F, 25., <cool2>
.
.
.
** Interaction: Cooling chanel_S14
*Sfilm
Cavity_tool-1.Section_14, F, 25., <cool14>
**
**
** OUTPUT REQUESTS
**
*Restart, write, frequency=0
**
** FIELD OUTPUT: F-Output-1
**
*Output, field, frequency=1
*Node Output
NT,
*Element Output, directions=YES
HFL,
*Contact Output
HFLA,
*Output, history, frequency=0
*End Step
** -----
**
**           C   Y   C   L   E           1
**
** -----
**
**-----
*** STEP:   I N J E C T I O N   F I X   T E M P E R A T U R E
**-----
**
*Step, name=Injection_Fixtemp_1, inc=10000000
*Heat Transfer, end=PERIOD, deltmx=5.
0.001, 0.001, 1e-07, 0.001,

```

## APPENDIX A. ABAQUS/STANDARD INPUT FILE

---

```
**
** BOUNDARY CONDITIONS
**
*Boundary
HDPE_Top, 11, 11, 180.
**
** INTERACTIONS
**
** Interaction: Cavity_Injection
*Model Change, type=CONTACT PAIR, add
HDPE_Top-1.Cavity_Surface_1, Cavity_tool-1.Cavity_Tool_Cavity_Surface
** Interaction: HDPE_Cap_Inner_Tool
*Sfilm
HDPE_Top-1.OffsetElements-Inner_Tool, F, 25., <injection>
**
** OUTPUT REQUESTS
**
*Restart, write, frequency=0
*Print, contact=YES
**
** FIELD OUTPUT: F-Output-1
**
*Output, field, frequency=1
*Node Output
NT,
*Element Output, directions=YES
HFL,
*Contact Output
HFLA,
*Output, history, frequency=0
*End Step
**
**-----
*** STEP:                I N J E C T I O N
**-----
**
*Step, name=Injection_1, inc=10000000
*Heat Transfer, end=PERIOD, deltmx=5.
0.001, 0.099, 9e-07, 0.099,
**
** BOUNDARY CONDITIONS
**
** Name: HDPE_Cavity_Injection Type: Temperature
*Boundary, op=NEW
** Name: Hot_Runner_Temp_1 Type: Temperature
*Boundary, op=NEW
HDPE_Hot_Runner_1-1.Temp_HR1, 11, 11, 200.
** Name: Hot_Runner_Temp_2 Type: Temperature
*Boundary, op=NEW
HDPE_Hot_Runner_2-1.Temp_HR2, 11, 11, 200.
** Name: Hot_Runner_Temp_3 Type: Temperature
```

APPENDIX A. ABAQUS/STANDARD INPUT FILE

---

```

*Boundary, op=NEW
HDPE_Hot_Runner_3-1.Temp_HR3, 11, 11, 200.
** Name: Hot_Runner_Temp_4 Type: Temperature
*Boundary, op=NEW
HDPE_Hot_Runner_4-1.Temp_HR4, 11, 11, 200.
**
** INTERACTIONS
**
** Interaction: HDPE_Cap_Inner_Tool
*Sfilm
HDPE_Top-1.OffsetElements-Inner_Tool, F, 25., <injection>
**
*End Step
**
**-----
*** STEP:                               S U B S T E P
**
**                               RAMP OF THE HEAT FLUX ON THE SURFACE
**
**                               FOR FURTHER REEDING: SECTION 21.2.4 V.6.5-1
**-----
**
*Step, name=Substep_1
*Heat Transfer, end=PERIOD, deltmx=5.
1e-05, 1e-05, 1e-10, 1e-05,
**
** INTERACTIONS
**
** Interaction: Cavity_Injection
*Model Change, type=CONTACT PAIR, remove
HDPE_Top-1.Cavity_Surface_1, Cavity_tool-1.Cavity_Tool_Cavity_Surface
**
*End Step
**
**-----
*** STEP:                               P R E S S I N G
**-----
**
*Step, name=Pressing_1, inc=10000000
*Heat Transfer, end=PERIOD, deltmx=5.
0.001, 0.16, 1.6e-07, 0.16,
**
** INTERACTIONS
**
** Interaction: Cavity_Pressing
*Model Change, type=CONTACT PAIR, add
HDPE_Top-1.Cavity_Surface_2, Cavity_tool-1.Cavity_Tool_Cavity_Surface_2
** Interaction: HDPE_Cap_Inner_Tool
*Sfilm
HDPE_Top-1.OffsetElements-Inner_Tool, F, 25., <pressing>
**

```

## APPENDIX A. ABAQUS/STANDARD INPUT FILE

---

```
*End Step
**
**-----
*** STEP:                S U B S T E P
**-----
**
*Step, name=Substep_2
*Heat Transfer, end=PERIOD, deltmx=5.
1e-05, 1e-05, 1e-10, 1e-05,
**
** Interaction: Cavity_Pressing
*Model Change, type=CONTACT PAIR, remove
HDPE_Top-1.Cavity_Surface_2, Cavity_tool-1.Cavity_Tool_Cavity_Surface_2
**
*End Step
**
**-----
*** STEP:                C O O L I N G
**-----
**
*Step, name=Cooling_1, inc=10000000
*Heat Transfer, end=PERIOD, deltmx=5.
0.001, 0.38, 3.8e-07, 0.1,
**
** INTERACTIONS
**
** Interaction: Cavity_Cooling
*Model Change, type=CONTACT PAIR, add
HDPE_Top-1.Cavity_Surface_3, Cavity_tool-1.Cavity_Tool_Cavity_Surface_3
** Interaction: HDPE_Cap_Inner_Tool
*Sfilm
HDPE_Top-1.OffsetElements-Inner_Tool, F, 25., <cooling>
**
*End Step
**
**-----
*** STEP:                S U B S T E P
**-----
**
*Step, name=Substep_3
*Heat Transfer, end=PERIOD, deltmx=5.
1e-05, 1e-05, 1e-10, 1e-05,
**
** Interaction: Cavity_Cooling
*Model Change, type=CONTACT PAIR, remove
HDPE_Top-1.Cavity_Surface_3, Cavity_tool-1.Cavity_Tool_Cavity_Surface_3
**
*End Step
**
**-----
*** STEP:                S Y S T E M   P R E P A R A T I O N
```

APPENDIX A. ABAQUS/STANDARD INPUT FILE

---

```
**-----  
**  
*Step, name=System_Preparation_1, inc=10000000  
*Heat Transfer, end=PERIOD, deltmx=5.  
0.001, 0.8, 8e-07, 0.1,  
**  
** INTERACTIONS  
**  
** Interaction: Cavity_System_Prep  
*Model Change, type=CONTACT PAIR, add  
HDPE_Top-1.Cavity_Surface_4, Cavity_tool-1.Cavity_Tool_Cavity_Surface_4  
** Interaction: HDPE_Cap_Inner_Tool  
*Sfilm  
HDPE_Top-1.OffsetElements-Inner_Tool, F, 25., <system_prep>  
**  
*End Step  
**  
**-----  
*** STEP:                S U B S T E P  
**-----  
**  
*Step, name=Substep_4  
*Heat Transfer, end=PERIOD, deltmx=5.  
1e-05, 1e-05, 1e-10, 1e-05,  
**  
** Interaction: System_Prep  
*Model Change, type=CONTACT PAIR, remove  
HDPE_Top-1.Cavity_Surface_4, Cavity_tool-1.Cavity_Tool_Cavity_Surface_4  
** OUTPUT REQUESTS  
**  
*Restart, write, frequency=0  
**  
*End Step  
**  
**-----  
**                C Y C L E      2  
**  
**-----  
.  
.  
.  
.  
.  
.  
.  
.  
.  
.  
.  
.  
**-----  
**
```



*APPENDIX A. ABAQUS/STANDARD INPUT FILE*

---

```
**           C   Y   C   L   E           10
**
** -----
** -----
**
**           E   N   D           A   N   A   L   Y   S
**
** -----
```